Effect of wind variability on dynamics of upwelling in vicinity of the Hel Peninsula (Gdansk Basin) in summer 1980

(hindcast modelling study) [a]

Andrzej Jankowski

Institute of Oceanology of PAS, Powstancow Warszawy 55, 81-712 Sopot, Poland

e-mail: jankowsk@iopan.gda.pl

Abstract

A three-dimensional baroclinic σ - coordinate model was applied to describe (study, investigate) the circulation and thermohaline variability in the coastal zone in the south-eastern Baltic Sea. The model is based on the **P**rinceton **O**cean **M**odel code of Blumberg & Mellor (1987), known as POM, and has horizontal resolution of ~ 5 km and 24 σ - levels in the vertical.

The hydrodynamic conditions and variability of seawater temperature and salinity in the coastal region off the Polish coast due to atmospheric forcing in summer 1980 are analyzed. The numerical simulations were performed with real atmospheric forcings for summer (July-August) 1980. Model results exhibit occurrence and development of an intense upwelling-like events in the area off the Hel Peninsula.

A comparison of computed and measured temperature and salinity shows that the model reproduces the vertical structure of seawater temperature and salinity in a good agreement to the *in situ* observations.

Abstract ... continued

The results of hindcast simulations show that under the real atmospheric forcing in summer period of 1980, near the southeastern Polish Baltic coast two upwelling-like events developed, one - very intensive, on 27 July - 03 August, and the weaker one, on 13-20 August and, as a result of these events the hydrological conditions in the coastal area off Wladyslawowo (the Hel Peninsula) were substantially modified.

The modelled time series of seawater temperature and salinity as well as time series of vertical component of currents velocity vector in the surface layer at the point **W** (Fig. 1) have showed high correlation with the temporal variability of the logitudinal component of the wind speed vector and the direction of the wind.

The lagged cross-correlation functions display some delay (2-4 days) in maximum values of the cross-correlation in the case of seawater temperature (positive correlation). Water salinity exibits high positive correlation with no delay in surface layer and weaker negative correlation with 2-5 days delay in the bottom layer. In the case of the vertical component of the current velocity vector correlation, correlations are negative and no delay may be observed.

The results of calculations showed correlations between the temporal variability of the sea level and seawater temperature and salinity at 4 points (**W1, H, L ,U**) (Fig. 1) in the coastal zone. These findings may be useful in a forecasting of the upwelling events as additional, regionally important, relationships besides used as the standard, dependence on atmospheric forcings.

1. Introduction

As usual upwelling occurs when cold water from the lower layers of the oceans is raised towards the surface. Wind-induced upwelling of cold water is a phenomenon often observed on the coasts of oceans, shelf seas and large inland waters (see e.g. Csanady 1982, Robinson 1985). It is generally assumed that Ekman offshore transport in the surface layer, generated by a longshore wind blowing with the coast to the left (in the northern hemisphere), is compensated by the upwelling of cold water.

A physical and theoretical description of upwelling can be found in e.g. Gill & Clarke (1974), Smith (1968), Gill (1982). The large scale wind induced (Ekman) upwelling is well known, for example, from off the west coasts of North and South America in the Pacific Ocean and off West and South Africa in the Atlantic on an oceanic scale (cf., e.g., Robinson 1985).

On a smaller scale wind-induced upwelling also occurs in a shelf semi-enclosed sea like the Baltic Sea. Lehmann and Myberg (2008) published comprehensive review of the upwelling, its dynamics and reflections to ecosystem processes in the Baltic Sea. Using all relevant literature they tried to close the gaps of our present knowledge on the Baltic Sea upwelling-like events and o some recommendations for future work have been outlined.

Due to its importance, a deeper understanding of the upwelling process and its implication on the marine environment allow to improve forecast of the local weather prediction as well as algae bloom forecasting, transports and mixing of nutrients and harmful substances. First activities in that direction have been undertaken and results of this work have been presented at the Baltic Sea Science Conference in March 1922, 2007 at Rostock University reported in Myrberg et al. (2008).

1. Introduction ... continued

Infrared satellite images provide compelling evidence for upwelling occurrence along the Baltic coast (Gidhagen 1984, 1998,Hansen et al. 1993, Siegel et al. 1994, Bychkova and Victorov 1987, Bychkova et al. 1988, Urbanski 1995, Krezel 1997). Upwelling events in the various parts of the Baltic have some specific features related to regional characteristics of bottom topography and shape of the coastline. Thus, the wind pattern favorable for the birth of upwelling depends on the local features.

Upwelling has been frequently studied at the Polish coast. Most often upwelling has been found to take place offshore Hel Peninsula (e.g. Matciak et al., 2001, Urbanski 1995, Krezel 1997). The upwelling of cold coastal water in the area off the open sea coast of the Hel Peninsula occurs each year, often during summer period (July - September).

Example of upwelling was reported by Malicki & Mietus (1994). The surface seawater temperature recorded in September 1989 at two coastal stations (off Kolobrzeg and Wladyslawowo) on the Polish coast exhibited a large upwelling-like fall (variations of the order 10 units (^{o}C)) and a duration of several days. This hydrological event was assumed to be related to the anemobaric situation obtaining in September 1989. Malicki & Mietus (1994) classified this anemobaric situation as typically causing a large fall in seawater surface temperature along the Polish Baltic coast.

According to Kreel et al. (2005), in the Hel area the upwelling region has a spatial range of 14 000 km^2 while in Leba area the range is 3500 km^2, that being at most 5000 km^2 in Kolobrzeg area. The temperature difference between upwelled deep water and surface water can reach 14 ^{o}C and the temperature gradient has a maximum value of 5 $^{o}C/km$ according to observations. The potential maximum area of upwelling along the Polish coast equal to 10 000 km^2 which is about 30% of the Polish economic zone (Kreel et al., 2005).

1. Introduction ... continued

There have been some *in situ* measurements and observations (Fennel & Seifert (1995), Fennel & Sturm (1992), Haapala (1994), Matciak *et al.* (2001), Schmidt *et al.* (1998), Svansson (1975)) of upwelling events occurring in different regions of the Baltic Sea. However, field data are not complete enough to allow description of the upwelling dynamics.

Hence, numerical simulations and modelling of specific hydrological situations with reasonable initial conditions, frequently used as basic tool, lead to an understanding of the dynamics of processes influencing circulation and thermohaline variability in the selected sea regions.

Several attempts have been made to investigate coastal upwelling phenomena in different regions of the Baltic Sea with 3-D numerical models (see e.g. Fennel and Seifert 1995, Lehmann et al. 2002, Myrberg & Andrejev 2003, Myrberg et al. 2010, Kowalewski 1998, Kowalewski and Ostrowski 2005, Zhurbas et al. 2004, Jankowski 2000, 2002).

In Jankowski (2002) upwelling was investigated under real anemobaric conditions in September 1989 and it was pointed out that the characteristic variability of wind field and the bottom topography variations as well as coastline favour upwelling water movements at the southeastern Polish Baltic coast. Along the Hel Peninsula specific conditions for the occurrence and development of upwelling-like processes were found.

1. Introduction ... continued

Main intention of this investigation is to verify these findings under different atmospheric conditions: i.e., real atmospheric conditions occured in summer 1980. Reported here hindcast numerical simulations were performed to reconstruct the hydrological conditions in the coastal area of the southeastern Baltic and related to the real atmospheric conditions in July and August 1980.

Main aims is to reconstruct hydrological situation and to find some relationships of calculated hydrological parameters with forcings (wind velocity and its direction) as well as relation between calculated (modelled) parameters: seawater temperature and salinity and sea level at the selected coastal stations.

The objective of this study is to describe results of model expriments that have been performed to investigate influence of the wind field variability on the dynamic processes related to upwelling-like events in the vicinity of the Hel Peninsula in summer period of 1980.

The 3-D (σ - coordinate) model has been used here for hindcast simulations. The model is based on the Princeton Ocean Model code of Blumberg & Mellor (1987) and Mellor (1993), known as POM and was adapted to the Baltic Sea conditions (Jankowski 2002). It is believed that the results of numerical simulations have supplied a new insight into the dynamics of the upwelling induced by real atmospheric forcing along the Polish Baltic coast.

The paper is arranged as follows. Section 2 presents basic information on model, initial fields, atmospheric forcings and model simulatios strategy. Then, in Section 3, some details of the validation of the model calculations are outlined. Section 4 gives the results of the numerical experiments and simulations together with a discussion of the model results. Finally, some conclusions are given in Section 5.

2. Model

A three-dimensional (sigma coordinate model), based on the Princeton Ocean Model (POM) code (Blumberg and Mellor 1987) adapted to the Baltic Sea was applied for hindcast modelling of the variability of hydrodynamic conditions in the southeastern Baltic Sea due to real anemobaric situation in July and August 1980.

The simulations were performed for the whole Baltic with a horizontal resolution of ca. 5 km and 24 sigma- levels in the vertical. Simplified boundary conditions of the radiation type were applied at the open boundary of the model in the Skagerrak. The model bottom topography was elaborated on the basis of data from Seifert and Kayser (1995).

The numerical simulations were initiated with the climatological distribution of temperature and salinity for July.
The initial 3-D fields of the seawater temperature and its salinity in July were constructed from the monthly mean (multi-year averaged) maps taken from Bock's (1971) and Lenz's (1971) atlases and additional available in situ data.

Model was driven by realistic atmospheric forcings (winds, atmospheric pressure and surface heat fluxes) calculated on the basis of meteorological data taken from BED (2000) for July and August 1980 and by climatological forcings and river inflows.

The river runoff rates of the 31 main rivers (assumed as yearly means) were taken into consideration.

2. Model ... continued

2.1 Model forcings

The wind fields were estimated from the atmospheric surface pressure charts.

Wind stress components and surface heat fluxes were estimated by the bulk formula (for details cf. Jankowski (2002)).

The climatological forcings were calculated in the following way.

The 2-D fields of the temperature (T) and salinity (S) at the sea surface for July and August were taken from the monthly mean (climatic) surface maps in Bock's (1971) and Lenz's (1971) atlases.

Next, the 2-D fields of T and S were linearly interpolated in time with an interval equal to the internal time step. The climatological forcings were coupled to the model by so-called method of relaxation towards climatology (cf. Lehmann 1995, Jankowski 2000, 2002).

2.2 Model simulations

The model simulations were performed in two stages.

The first step, pre-processing run, was used to initialize the model computations.

At this stage the model started from the three-dimensional initial distribution of temperature and salinity and was forced only by the climatological forcings, without external atmospheric forcing.

The initial fields of sea level, the current velocity vector components and the mean-depth current components were set equal to 0.

An adaptation of the model dynamics to the initial fields and climatology was achieved by a forward integration of the model equations over a period of 20 days after which a quasi-stationary state was reached.

The second stage was started from the previous step's final results and consisted of a fully prognostic run. Besides climatological forcings, the model was now forced by real atmospheric forcings (atmospheric pressure, winds and heat fluxes) for a period of 62 days (01 July to 31 August 1980).

In the simulation presented here, the surface salinity flux at the sea surface was assumed to be negligible and was set equal to 0.

3. Model validation

In order to test the reliability of the model calculations, the results were compared with the in situ measurements (vertical sounding of temperature and salinity at a number (five) hydrographic stations **S1, S2, S3, S4, S5** in the Southern Baltic (taken from the ICES Oceanographic Database and Service (http://www.ices.dk/ocean).

Their distribution in the Baltic Sea is shown in Fig. 1. The hydrographic stations chosen for the model verification, represent thermohaline variability in relation to different bathymetric conditions in the southern Baltic.

For the purpose of visualization the model results were interpolated by cubic spline (Forsythe *et al.*, 1977) from σ - levels onto "z" - levels with a space step equal to 2 m.

Figure 2 depicts vertical profiles of the modelled sea water temperature and salinity at five points **S1** - **S5** for period of 17-27 July 1980. Besides the model results, the figure also shows the *in situ* measured temperature and salinity profiles.

In order to evaluate quantitative model results versus *in situ* observations standard statistical criteria were calculated: (i) the correlation coefficient (cor), (ii) the average error (ae), (iii) the average absolute error (aae), (iv) the root mean squared error ($rmse$), (v) the model efficiency coefficient (ef), (vi) the relative mean squared residual error ($rmsre$), (vii) the ratio of average values (sws) and (viii) the special correlation coefficient (rs), frequently used in ecological and hydrological modelling (cf. e.g. Mayer & Butler 1993, Ozga-Zieliska & Brzeziski 1997). Some details on the formula to calculate them can be found in **Appendix**.

3. Model validation ... continued

The estimates of all above mentioned statistical criteria for the temperature and salinity profiles in selected points **S1-S5** (cf. Fig. 1) are presented in Tabs. 1 and 2, where, in addition, estimates of the determination coefficient $cov2$ equal to the squarred value of the correlaton coefficient cov have been shown.

Comparison of the computed and measured temperature and salinity vertical profiles shows (cf. Fig. 2) that the model reproduces the vertical structure of seawater temperature and salinity in relatively good agreement with the *in situ* observations.

The results depicted in Figs. 2 and the estimates of statistical criteria presented in Tabs.1 and 2 show that a degree of agreement between observations and computed data depends on the regional scale of bottom structures (location of observation point).

In general, the model produces acceptable vertical profiles of the seawater temperature and its salinity. The profiles variability in time is similar to *in situ* measured data. Thus the model results may be used for a more detailed analysis of the water dynamics in the south-eastern Baltic Sea.

4. Results of simulations

The hindcast calculations were performed along with the methodology and strategies decribed in the previous section.

Although model runs were performed for the entire Baltic Sea, the presentation of the hindcast simulation results is limited to the coastal area along the south-eastern part of the Polish Baltic coast (15^o 00'E-20^o 06'E; 54^o 00'N-55^o 48'N) (cf. Fig. 1).

Fig. 3 illustrates exemplary time series of wind direction, wind speed and calculated seawater temperature and salinity and vertical component of current velocity in surface layer at selected depths at point **W** (off Wladyslawowo, see Fig. 1 for point location). From this figure it follows that an intense upwelling-like event occurrs on days 27-33 of simulations (from 27 July to 02 August 1980) and less intense one, occurs on days 45-50 of model simulations, i.e., from 13th to 20 August 1980.

All of them are related to characteristic anemobaric situations: rapid changes in wind velocity and in wind direction to upwelling favourable (winds from N-E sector). The maximum of upwelling event occurrs 3-4 days after. It is worth to notice, that during the both two upwelling-like events wind velocity was almost constant (ca. 10 m/s).

4. Results of simulations ... continued

The response of stratified sea water to upwelling favourable winds in sea surface temperature and salinity are shown in Figs. 4 and 5. Snapshots of surface temperature and water salinity at 10 m depth on eight succesive days depict development of the stronger upwelling event (on 27 July to 03 August). To ilustrate variability of water dynamics in the surface layers the currents velocity vector calculated at depth of 10 m have been added to Figs. 4-5.

The figures demonstrate the temporal history of the occurrence of coastal upwelling, its evolution and its disappearance in the vicinity of the south-eastern Polish coast of the Balitc. Peak upwelling response in the surface seawater temperature fields (as with salinity field) appears on days 30-31 of modeling time period, i.e., on 30-31 July 1980.

To complete description of this hydrological event, the anemobaric situation related to time period of event was reproduced in Fig. 6 based on meteorological data from BED (2000).

The next figures, Figs. 7-9 display the development of the weaker upwelling-like event (on 13 to 20 August 1980) as well as anemobaric situation assmed to be related to.

4. Results of simulations ... continued

The above figures demonstrate the temporal history of the occurrence of coastal upwelling-like events, their evolution and disappearence in the southern Baltic along the Polish coast in July and August 1980.

The simulated circulation patterns complete the spatial picture of hydrodynamic conditions related to the upwelling-like events. Current vectors at 10 m depth illustrate the overall picture and the variability of water exchange between the coastal zone and the open sea related to the variability of forcing.

It is straightforward matter to discover from the above figures that the evolution of dynamic situation is closely related to the variability of atmospheric forcing (wind direction).

Analysis of the above figures confirms that not only the subtleties of the bottom topography but also the shoreline configuration relative to the wind direction contribute to the variability in sea water temperature and circulation patterns.

The results of hindcast simulations show that under real atmospheric forcing in summer of 1980, near the Polish Baltic coast an intensive time-variable upwelling-like process developed, as a result of which the hydrological conditions in the coastal area were substantially modified.

4. Results of simulations ... continued

Figurs 10a-c present time series of the longitudinal component of the wind vector speed (u) [m/s] and wind direction [^{o}] and modelled timee series of seawater temperature T [^oC], its salinity S [psu] nd timee series of the vertical component of currents velocity vector w [cm/s] at selected depths in the point **W**, (total depth equal to 18 m), off Wladyslawowo (location of point is shown in Fig. 1).

From these figures it follows that the timing of both observed upwelling-like events (27-33 and 45-50 days of simulations, respectively (cf. Fig. 3, 4-5, 7-8), is close related to specific variability of the longitudinal component of the wind speed vector as well as of its direction.

The next figures, Figure 11a-b display the course of lagged cross-corelation functions between the wind component u and wind direction with the modelled hydrological parameters T, S, w at all depths from surface to the bottom (at depths 0-16 m).

The estimates of values of the cross-correlation functions cor at lag equal to 0 days as well as their maximum value cor_{max} and the appropriate value of lag of its occurence have been presented in Table 3.

4. Results of simulations ... continued

From the above presented results (Figures 10 and 11) and Table 3, it follows that the modelled temporal evolution of seawater temperature, salinity and vertical component of currents velocity vector in the point **W** have showed good and significant correlation ($cov \geq \pm 0.195(0.254)$)at the 5% (1 %) level of significance [a]) with the temporal variability of the logitudinal component of the wind speed vector as well as with the direction of the wind.

The lagged cross-correlation functions exhibit some delay of 2-4 days in ocurrence of its maximum value in the case of seawater temperature (positive correlation at all depths).

In the case of salinity the highest and positive values of *cor* have been found in the surface layer (2-6) without any delay. Negative and smaller values of *cor* and cor_{max} have been seen at higher depths (6-16 m).

In the case of the vertical component of the current velocity vector correlation, correlations are negative and no delay may be observed.

---

[a] after (Emery & Thomson 1998)

4. Results of simulations ... continued

Figures 12a-d present evolution of the modelled sea level η $[cm]$ and time series of seawater temperature T $[^oC]$ and salinity S $[psu]$ at selected depths in the 4 coastal points **W1, L, U, H** (see Fig. 1 for their location).

Visual correlation between η and both termohaline parameters have been easily seen at all depths.

These foundings have been supported by values of estimated correlation coefficients: $cov_{T\eta}, cov_{S\eta}$, presented in Table 4.

The values of the correlation coefficient greater than $\pm$ 0.195 (0.254) are significant at the 5 % (1 %) level of significance (after Emery & Thomson 1998).

These results may be useful in a prognosis of the upwelling events as additional, regionally important, relationships besides used as the standard, dependence on winds variability.

5. Final remarks (Conclusions)

The 3-D circulation baroclinic model of the Baltic Sea, based on the Princeton Ocean Model code was applied to investigate water circulation and thermohaline variability in July and August 1980.

The results of hindcast simulations show that under the real atmospheric forcing in summer period of 1980, near the southeastern Polish Baltic coast two upwelling-like events developed, one - very intensive, on 27 July - 03 August, and the weaker one, on 13-20 August.

As a result of these events the hydrological conditions in the coastal area off Wladyslawowo (the Hel Peninsula) were substantially modified.

Specific conditions for the occurence and development of the upwelling processes in this area are observed. The results of present investigations confirm peculiar features of hydrodynamics in the region of the Hel Peninsula.

5. Final remarks (Conclusions) ... continued

The modelled time series of seawater temperature and salinity as well as time series of vertical component of currents velocity vector in the surface layer at the point **W** have showed high correlation with the temporal variability of the logitudinal component of the wind speed vector and the direction of the wind.

The lagged cross-correlation functions display some delay (2-4 days) in maximum values of the cross-correlation in the case of seawater temperature (positive correlation). Water salinity exibits high positive correlation with no delay in surface layer and weaker negative correlation with 2-5 days delay in the bottom layer. In the case of the vertical component of the current velocity vector correlation, correlations are negative and no delay may be observed.

The results of calculations showed the good correlation between the temporal variability of the sea level and seawater temperature and salinity at four points (**W1, H, L ,U**) in the coastal area. These findings may be useful in a forecasting of the upwelling events as additional, regionally important, relationships besides used as the standard, dependence on atmospheric forcings.

References

BED, (2000), *Atmospheric inputs.*, [in:] *The BED database*, http://data.ecology.su.se/Models/bedcontent.htm

Blumberg, A. F., Mellor G. L., (1987),*A description of a three-dimensional coastal ocean circulation model.*, [in:] *Three-Dimensional Coastal ocean Models.*, edited by N. Heaps, 208 pp., American Geophysical Union.

Bychkova I.A., Viktorov S.V., Shumakher D.A., (1988), *A relationship between the largescale atmospheric circulation and the origin of coastal upwelling in the Baltic Sea.*, Meteorol. Gidrol., 10, 91-98, (in Russian)

Bychkova I.A., Viktorov S.V., (1987),*Elucidation and systematization of upwelling zones in the Baltic Sea based on satellite data.*, Okieanologiya, 27, 218-223, (in Russian).

Bock K.H., (1971), *Monatskarten des Salzgehaltes der Ostsee, dargestellt fur verschiedene Tiefenhorizonte.*, Dt. hydrogr. Z., Erg.H. R.B., 12, Hamburg, 1-148

Csanady, G.T., (1982), *Circulation in the Coastal Ocean*, D. Reidel Publishing Co., Boston, MA, 279 pp.

Emery, W.J., & R.E. Thomson, 1998,*Data Analysis Methods in Physical Oceanography.* Pergamon Press, Oxford. 634pp.

Fennel W., Sturm M., (1992), *Dynamics of the western Baltic*, J. Mar. Sys., **3**, 183-205.

Fennel W., Seifert T., (1995, *Kelvin wave controlled upwelling in the western Baltc*, J. Mar. Sys., 6, 286-300.

Fennel W., Seifert T., 1995, *Kelvin wave controlled upwelling in the western Baltc*, J. Mar. Sys., 6, 286-300.

Gidhagen L., (1984), *Coastal upwelling in the Baltic Sea.*, Proc. 14th Conf. Baltic Oceanographers, Gdynia, vol. 1, 182-190

Gidhagen, L., (1987), *Coastal Upwelling in the Baltic Sea satellite and in situ measurements of sea-surface temperatures indicating coastal upwelling.* Estuarine, Coastal and Shelf Science 24, 449362.

Gill A.E., 1982, *Atmoshere-Ocean Dynamics*, Academic Press, New York, 662 pp.

Gill, A.E. and A.J. Clarke, 1974, *Wind-induced upwelling, coastal currents and sea-level changes*, Deep-Sea Res., 21, 325-345.

References .... continued

Haapala J., (1994), *Upwelling and its influence on nutrient concentration in the coastal Area of the Hanko Penisula, Entrance of the Gulf of Finland*, Estuar., Coast. Shelf Sci., 38, 507-521

Hansen L., Højerslev N.K., Soogaard H., (1993), *Temperature monitoring of the Danish marine environment and the Baltic Sea*, Københavns Universitet, Report 52, 77 pp.

Jankowski A., (2000), *Wind induced variability of hydrological parameters in the coastal zone of the Southern Baltic Sea numerical study.*, Oceanological Studies, XXIX, No. 3, 5-34

Jankowski A., (2002), *Variability of coastal water hydrodynamics in the Southern Baltic hindcast modelling of an upwelling event along the Polish coast.*, Oceanologia., 44 (4), 395-418.

Kowalewski M., (1998), *Coastal upwellings in a shallow stratified sea, for example, in the Baltic Sea.*, PhD thesis, University of Gdansk, Gdynia, 85 pp., (in Polish).

Kowalewski,M., Ostrowski,M., (2005), *Coastal up- and downwelling in the southern Baltic.* Oceanologia 47 (4), 453475.

Krezel A., 1997, *Recognition of mesoscale hydrophysical anomalies in a shallow sea using broadband satelitte teledetection methods*, Wydawnictwo Uniwersytetu Gdaskiego, Gdask, 173 pp. (in Polish).

Krezel, A., M. Ostrowski, M., Szymelfenig, (2005), *Sea surface temperature distribution during upwelling along the Polish Baltic coast.* Oceanologia, 47 (4), 415432.

Large W. G., Pond S., (1981), *Open ocean momentum flux measurements in moderate to strong winds*, J. Phys. Oceanogr., vol. 11, 324-336

Lehmann A., (1995),*A three-dimensional baroclinic eddy-resolving model of the Baltic Sea.*, Tellus, 47A, 1013-1031.

Lehmann, A., W. Krauss, H.-H. Hinrichsen, (2002), *Effects of remote and loc atmospheric forcing on circulation and upwelling in the Baltic Sea*, Tellus 54A (3), 299316.

Lenz W., (1971), *Monatskarten der Temperatur der Ostsee, dargestellt fur verschiedene Tiefenhorizonte.*, Dt. hydrogr. Z., Erg.H. R.B., 11, Hamburg, 1-148.

References .... continued

Matciak M., Urbanski J., Piekarek-Jankowska H., Szymelfenig M., (2001), *Presumable groundwater seepage influence on the upwelling events along the Hel Peninsula.*, Oceanological Studies, 30 (34), 125-132.

Malicki J, Mitus M., (1994), *Climate.*, [In:] *The Baltic Sea Atlas.*, A. Majewski and Z. Lauer (Eds.), IMGW, Warsaw, 60 69, (in Polish).

Mayer D.G., D.G. Butler, (1993), *Statistical validation*, Ecol. Modelling, 68, 21-32.

Myrberg, K., Andrejev, O., (2003), *Main upwelling regions in Baltic Sea statistical analysis based on three-dimensional modelling.* Boreal Environment Research 8, 97112.

Myrberg, K., Andrejev, O.. and Lehmann A., (2010), *Dynamic features of successive upwelling events in the Baltic Sea - a numerical case study*, Oceanologia, 52(1), 77-99.

Myrberg, K., Lehmann, U., Raudsepp, U., Szymelfenig, M., Lips, I., Lips, U, Matciak,M., Kowalewski,M.,Krezel,A., Burska,D., Szymanek, L.,Ameryk, A Bielecka, L., Bradtke, K., Gakowska, A., Gromisz, S., Jedrasik, J., Kaluzny, M Kozlowski, L., Krajewska-Soltys, A., Oldakowski, B., Ostrowski,M., Zalewski M., Andrejev, O., Suomi, I., Zhurbas, V., Kauppinen, O.-K., Soosaar, E Laanemets, J., Uiboupin, R., Talpsepp, L., Golenko, M., Golenko, N., Vahter E., (2008), *Upwelling events, coastal offshore exchange, links to biogeochemical processes Highlights from the Baltic Sea Science Conference March 19 22, 2007 at Rostock University.* Oceanologia 50 (1), 95113.

Ozga-Zielinska M., J. Brzezinski, (1997), *Applied hydrology*, PWN, Warszawa, 324pp, (in Polish).

Robinson I.S., (1985), *Satellite oceanography: an introduction for oceanographers and remote-sensing scientists*, Ellis Horwood Limited, Chichester, 455 pp.

Schmidt M., Seifert T., Lass H.-U., Fennel W., (1998), *Patterns of salt propagation in the South-western Baltic Sea*, Deutsche Hydrographische Zeitschrift, **50**, 345-364.

Seifert T., Kayser, B., (1995), *A high resolution spherical grid topography of the Baltic Sea.*, Meereswissenschaftliche Berichte, No. 9, Institut fur Ostseeforschung, Warnemunde, 72-88

References .... continued

Siegel H., Gerth M., Rudloff R., Tschersich G., 1994, *Dynamic features in the western Baltic Sea investigated using NOAA - AVHRR Data*, Dt. hydrogr. Z., 46, 191-209.

Smith, R.L., (1968), *Upwelling.*, Oceanography and Marine Biology, Annual Reviews, 6, 11-46.

Svansson A., (1975), *Interaction between the coastal zone and the open sea*, Finnish Mar. Res., 239, 11-28.

Urbanski J.,(1995), *Upwellings along the Polish coasts of the Baltic Sea*, Przegl. Geofiz., 40, 141-153, (in Polish).

Zhurbas V., T Stipa, P. Mälkki, T. Paka, N. Kuzmina., V. Sklyarov,(2004), *Mesoscale variability of the upwelling in the Southeastern Baltic Sea: IR images and Numerical Modelling*, Okeanologija 44, (5), 660-669 (in Russian).

Appendix

The selected statistical criteria , frequently used in hydrological and ecological modelling (cf. e.g. Mayer & Butler 1993, Ozga-Zieliska & Brzeziski 1997).

(i) the correlation coefficient **cor**:

$$cor = \frac{\sum_{i=1}^{N}(Y_{p,i} - \overline{Y}_p)(Y_{m,i} - \overline{Y}_m)}{\sqrt{\sum_{i=1}^{N}(Y_{m,i} - \overline{Y}_m)^2 \sum_{i=1}^{N}(Y_{p,i} - \overline{Y}_p)^2}}$$

(ii) the average error **ae**:

$$ae = \frac{1}{N}\sum_{i=1}^{N}(Y_{p,i} - Y_{m,i}) = \overline{Y}_p - \overline{Y}_m$$

(iii) the average absolute error **aae**:

$$aae = \frac{1}{N}\sum_{i=1}^{N} \mid (Y_{p,i} - Y_{m,i}) \mid$$

Appendix ... continuated

(iv) the root mean squared error **rmse**:

$$rmse = \sqrt{\frac{1}{N}\sum_{i=1}^{N}(Y_{p,i} - Y_{m,i})^2}$$

(v) the model efficiency coefficient **ef**:

$$ef = 1 - \frac{\sum_{i=1}^{N}(Y_{m,i} - Y_{p,i})^2}{\sum_{i=1}^{N}(Y_{p,i} - \overline{Y}_p)^2}$$

(vi) the relative mean squared residual error **wbr**:

$$wbr = \frac{100\%}{\overline{Y}_p}\sqrt{\frac{1}{N}\sum_{i=1}^{N}(Y_{m,i} - Y_{p,i})^2}$$

Appendix ... continuated

(vii) the ratio of average values **sws**:

$$sws = \frac{\overline{Y}_m}{\overline{Y}_p}$$

(viii) the special correlation coefficient **rs**:

$$rs = \sqrt{\frac{\sum_{i=1}^{N}(2\,Y_{m,i}Y_{p,i} - Y_{p,i}^2)}{\sum_{i=1}^{N} Y_{p,i}^2}}$$

where:
N - number of measurement levels in the vertical profile,
$\overline{Y}_m, \overline{Y}_p$ - the depth-mean of $Y_{m,i}, Y_{p,i},\ i = 1, ..., N$), respectively;
$Y_{m,i}, Y_{p,i}$ - the ith of N modelled and *in situ* measured temperature or salinity at ith - level, repectively.

Tables

Table 1 Values of statistical criteria calculated for verification of modelled temperature profiles in selected points in the south-eastern Baltic Sea. See text and **Appendix** for more detail explanations

St.	aae	ae	cor	ef	rmse	rs	sws	wbr	cor2
	[°]	[°]	[-]	[-]	[°C]	[-]	[-]	[%]	[%]
S1	1.23	0.88	0.936	0.84	2.04	0.97	1.15	31.7	87.6
S1	1.68	1.66	0.948	0.78	2.32	0.96	1.40	51.2	89.9
S1	2.56	2.56	0.929	0.59	3.31	0.92	1.40	51.2	86.3
S1	2.18	2.09	0.950	0.72	2.80	0.94	1.33	43.8	90.2
S2	0.89	0.65	0.976	0.93	1.20	0.99	1.10	18.5	95.3
S2	1.51	1.38	0.927	0.76	2.16	0.96	1.23	36.5	85.9
S2	1.54	1.52	0.937	0.76	2.17	0.96	1.25	36.1	87.8
S2	1.52	1.46	0.929	0.76	2.23	0.96	1.24	37.1	86.3
S2	1.25	1.19	0.959	0.85	1.77	0.97	1.19	28.8	92.0
S2	1.34	1.16	0.958	0.86	1.77	0.97	1.19	29.0	91.8
S2	1.05	0.86	0.968	0.90	1.53	0.98	1.14	24.3	93.7
S2	1.19	0.93	0.961	0.89	1.68	0.98	1.15	26.9	92.4
S3	1.17	-0.98	0.969	0.87	1.80	0.98	0.85	27.5	93.9
S4	0.66	0.58	0.984	0.95	1.00	0.99	1.09	16.1	96.8
S5	0.63	-0.26	0.980	0.96	0.83	0.99	0.96	12.6	96.0
S5	0.63	0.47	0.990	0.97	0.73	1.00	1.08	12.2	98.0
S5	0.72	0.26	0.983	0.96	0.81	0.99	1.04	13.0	96.6
S5	0.60	0.39	0.992	0.97	0.71	1.00	1.06	11.5	98.4
S5	0.87	0.39	0.983	0.96	0.93	0.99	1.06	15.0	96.8
S5	0.78	0.12	0.982	0.96	0.97	0.99	1.02	15.0	96.4
S5	1.01	-0.47	0.981	0.90	1.48	0.98	0.93	21.8	96.2
S5	0.80	0.58	0.990	0.96	0.90	0.99	1.09	14.4	98.0
S5	1.47	1.03	0.970	0.86	1.67	0.97	1.18	29.4	94.1
S5	1.22	0.85	0.984	0.91	1.36	0.98	1.14	22.9	96.8
S5	1.07	0.65	0.983	0.92	1.24	0.99	1.11	20.8	96.6
S5	1.11	0.72	0.976	0.92	1.28	0.98	1.12	21.7	95.3
S5	1.15	0.12	0.981	0.92	1.31	0.98	1.02	21.0	96.2

Table 2 Values of statistical criteria calculated for verification of modelled salinity profiles in selected points in the south-eastern Baltic Sea. See text and **Appendix** for more detail explanations

St.	aae	ae	cor	ef	rmse	rs	sws	wbr	cor2
	[psu]	[psu]	[-]	[-]	[psu]	[-]	[-]	[%]	[%]
S1	0.22	-0.19	0.994	0.88	0.38	1.00	0.98	4.6	98.8
S1	0.25	-0.20	0.982	0.74	0.33	1.00	0.98	4.0	96.6
S1	0.49	-0.49	0.998	0.41	0.77	1.00	0.94	9.2	99.6
S1	0.27	-0.26	0.977	0.79	0.40	1.00	0.97	4.9	95.5
S2	0.39	-0.39	0.993	0.93	0.52	1.00	0.96	5.5	97.9
S2	0.31	-0.31	0.992	0.95	0.45	1.00	0.97	4.8	98.4
S2	0.24	-0.22	0.996	0.98	0.30	1.00	0.98	3.2	99.2
S2	0.42	-0.42	0.983	0.91	0.59	1.00	0.96	6.1	96.6
S2	0.28	-0.28	0.994	0.96	0.39	1.00	0.97	4.2	98.8
S2	0.32	-0.21	0.990	0.96	0.41	1.00	0.98	4.3	99.6
S2	0.32	-0.17	0.985	0.96	0.43	1.00	0.98	4.5	97.0
S2	0.32	-0.19	0.986	0.96	0.43	1.00	0.98	4.5	97.2
S3	0.31	-0.30	0.971	0.91	0.53	1.00	0.97	5.8	94.3
S4	0.20	-0.07	0.988	0.97	0.26	1.00	0.99	3.0	97.6
S5	0.45	0.18	0.980	0.92	0.58	1.00	1.02	6.1	96.0
S5	0.48	0.11	0.988	0.94	0.54	1.00	1.01	5.6	97.6
S5	0.53	0.22	0.994	0.92	0.62	1.00	1.02	6.4	98.8
S5	0.56	0.22	0.986	0.92	0.67	1.00	1.02	6.9	97.2
S5	0.46	0.13	0.994	0.96	0.50	1.00	1.01	5.0	98.8
S5	0.46	0.08	0.995	0.96	0.51	1.00	1.01	5.1	99.0
S5	0.34	-0.23	0.990	0.97	0.43	1.00	0.98	4.4	98.0
S5	0.60	0.15	0.930	0.86	0.78	1.00	1.02	8.3	86.5
S5	0.78	0.60	0.939	0.75	1.13	0.99	1.06	11.9	88.2
S5	0.77	0.59	0.961	0.80	1.06	0.99	1.06	11.1	92.4
S5	0.57	0.38	0.992	0.91	0.70	1.00	1.04	7.1	98.4
S5	0.55	0.36	0.989	0.90	0.75	1.00	1.04	7.6	97.8
S5	0.57	0.34	0.994	0.91	0.72	1.00	1.03	7.2	98.8

Table 3

Cross-correlation coefficients *cor* and cor_{max} between time-series of the longitudinal component of the wind vector speed (u) and wind direction and timee series of modelloed water temperature, salinity and the vertical component of the velocity vector for the current at the selected depths at the monitoring point **W**, off Wladyslawowo. In parentheses is the value of the delay(lag) (in days) for which the cross-correlation function approaches its extreme value. The calculation was carried out with the real forces forcing fields.

Depth	Temperature		Salinity		Vertical component of current velocity vector	
[m]	*cor*	cor_{max}	*cor*	cor_{max}	*cor*	cor_{max}
			Longitudinal component of the wind vector speed			
0.0	0.033	0.293 (8.5)	0.723	0.723 (0.0)	0.570	0.570 (0.0)
2.0	0.110	0.348 (7.5)	0.714	0.714 (0.0)	-0.793	-0.793 (0.0)
4.0	0.233	0.422 (6.5)	0.613	0.613 (0.0)	-0.838	-0.838 (0.0)
6.0	0.358	0.497 (4.5)	0.410	0.410 (0.0)	-0.850	-0.850 (0.0)
8.0	0.462	0.560 (4.0)	0.119	-0.196 (8.0)	-0.860	-0.860 (0.0)
10.0	0.512	0.581 (3.5)	-0.087	-0.292 (4.5)	-0.861	-0.861 (0.0)
12.0	0.552	0.596 (2.0)	-0.222	-0.363 (4.0)	-0.875	-0.875 (0.0)
14.0	0.593	0.627 (1.5)	-0.330	-0.431 (3.5)	-0.885	-0.885 (0.0)
16.0	0.598	0.636 (1.5)	-0.366	-0.465 (2.5)	-0.891	-0.891 (0.0)
			Wind direction			
0.0	0.055	0.192 (8.5)	0.440	0.440 (0.0)	0.446	0.446 (0.0)
2.0	0.101	0.239 (6.0)	0.432	0.432 (0.0)	-0.558	-0.558 (0.0)
4.0	0.163	0.311 (5.5)	0.360	0.360 (0.0)	-0.576	-0.576 (0.0)
6.0	0.246	0.358 (4.5)	0.215	0.215 (0.0)	-0.570	-0.570 (0.0)
8.0	0.328	0.400 (3.5)	0.008	-0.182 (4.5)	-0.553	-0.553 (0.0)
10.0	0.360	0.412 (2.0)	-0.139	-0.263 (3.0)	-0.535	-0.535 (0.0)
12.0	0.393	0.429 (1.5)	-0.224	-0.317 (2.0)	-0.531	-0.531 (0.0)
14.0	0.431	0.458 (1.0)	-0.292	-0.357 (1.5)	-0.500	-0.500 (0.0)
16.0	0.437	0.462 (1.0)	-0.302	-0.353 (1.5)	-0.487	-0.487 (0.0)

Table 4
Correlation coefficient $cor_{T\eta}$ i $cor_{S\eta}$ between the modelled time series of sea level η and time series of seawater temperature (T) and salinity (S) at the selected depths in the four points located in the coastal zone: **W1** (15 m), **U** (15 m), **L** (15 m), **H** (30 m). In parentheses is shown the bottom depth in the point location.

	Sta.	$cor_{T\eta}$	$cor_{S\eta}$	Depth	Sta.	$cor_{T\eta}$	$cor_{S\eta}$
1 (0.025m)	**L**	0.113	-0.268	1 (0.025m)	**U**	0.177	-0.271
3 (0.14m)		0.126	-0.268	3 (0.14m)		0.185	-0.271
5 (0.56m)		0.159	-0.268	5 (0.56m)		0.205	-0.272
10 (4.3m)		0.321	-0.288	10 (4.3m)		0.283	-0.280
15 (8.3m)		0.394	-0.334	15 (8.3m)		0.274	-0.301
20 (12.2m)		0.422	-0.391	20 (12.2m)		0.254	-0.351
23 (14.6m)		0.432	-0.406	23 (14.6m)		0.252	-0.386
1 (0.05m)	**H**	-0.076	0.286	1 (0.025m)	**W1**	0.126	0.365
3 (0.28m)		-0.066	0.286	3 (0.14m)		0.144	0.365
5 (1.1m)		-0.029	0.289	5 (0.56m)		0.198	0.359
10 (8.7m)		0.193	0.185	10 (4.3m)		0.436	0.075
15 (16.6m)		0.365	-0.163	15 (8.3m)		0.530	-0.239
20 (24.5m)		0.397	-0.376	20 (12.2m)		0.510	-0.348
23 (29.2m)		0.302	-0.352	23 (14.6m)		0.478	-0.334

Figures

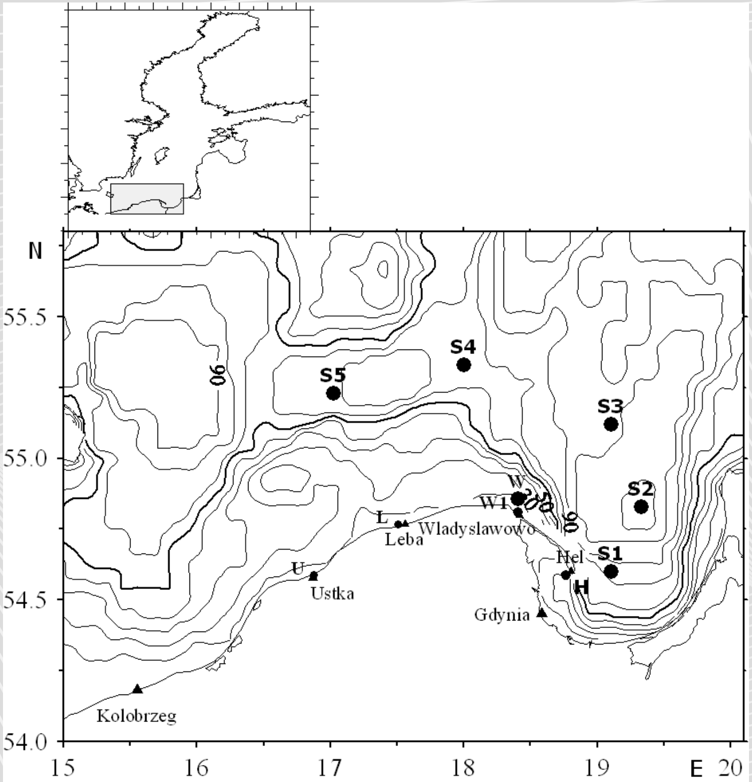

Figure 1 The study area and location of points used for verification of the model calculations: **S1-S5** and to visualize the results of calculations: **W, W1, H, L, U** - Wladyslawowo (**W, W1**), Hel (**H**), Leba (**L**) and Ustka (**U**), respectively; Bottom topography was elaborated based on data from Seifert and Kayser (1995). The numbers on the isolines indicate the depth in meters.

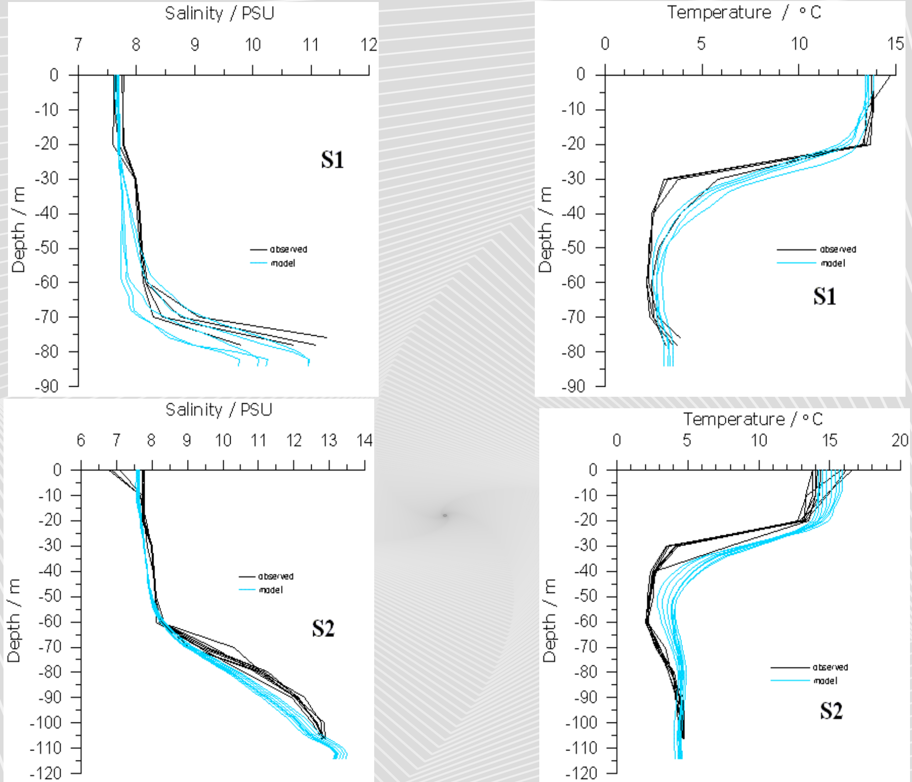

Figure 2a Modelled and in situ measured vertical distributions of temperature [^oC] and salinity [psu] at the hydrographic stations **S1** and **S2**. For details of their locations, see Fig. 1

Home Page
Title Page
Contents
Page 35 of 62
Go Back
Full Screen
Close
Quit

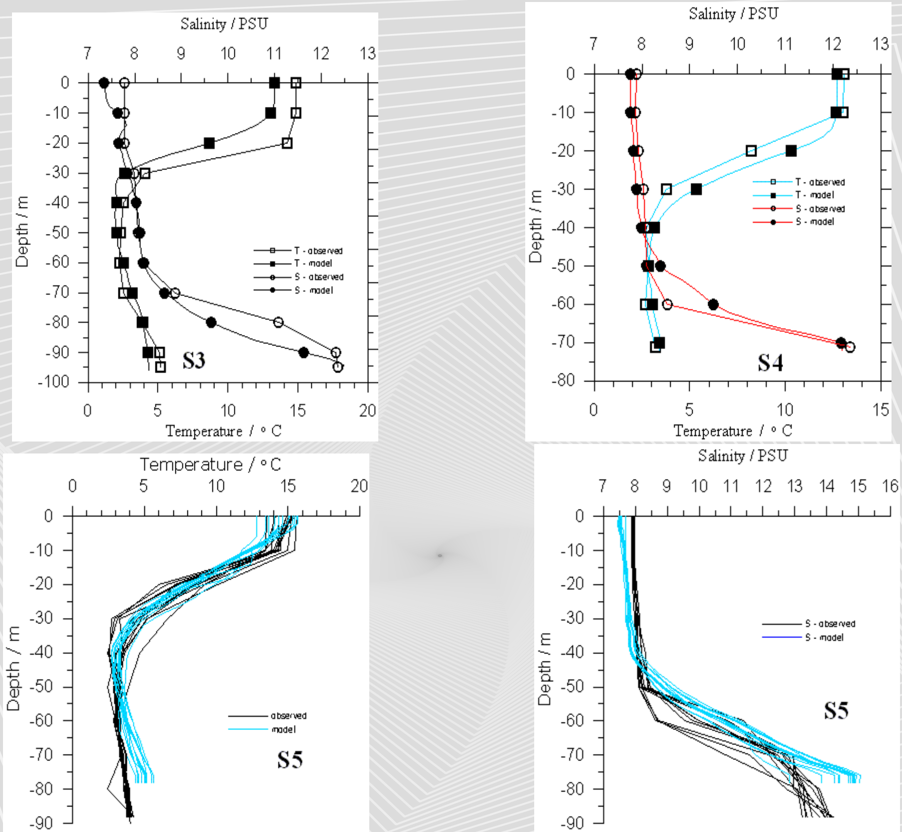

Figure 2b Modelled and in situ measured vertical distributions of temperature [^oC] and salinity [psu] at the hydrographic stations **S3**, **S4** and **S5**. For details of their locations, see Fig. 1

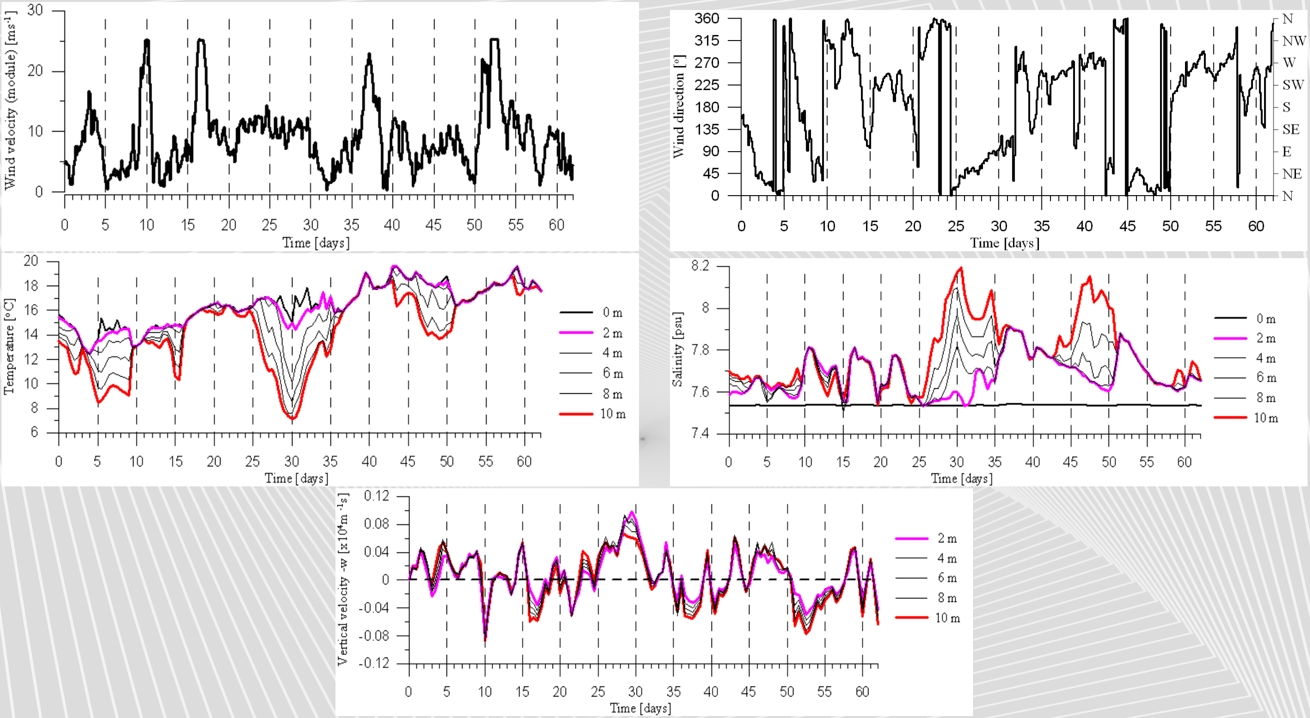

Figure 3 Time evolution of wind direction [^{o}], wind velocity [m/s], the simulated seawater temperature (T) [^oC], salinity (S) [psu] and the vertical component of the currents velocity vector (w) [cm/s] at point **W** in the vicinity of the Hel Peninsula. Location of point see Fig. 1

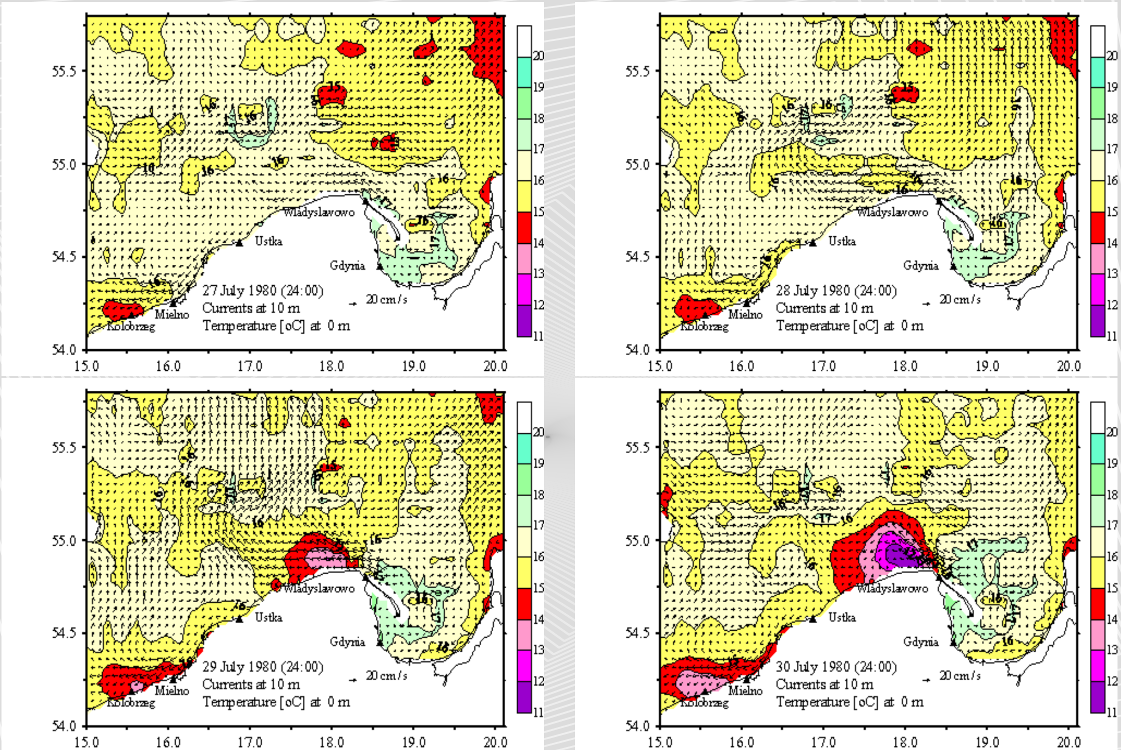

Figure 4 Simulated sea water temperature $[^oC]$ in surface layer and currents vector $[cm/s]$ at 10 m depth in a time sequence of 1 day from 27.07.1980 to 03.08.1980.

Home Page
Title Page
Contents
◀◀ ▶▶
◀ ▶
Page 38 of 62
Go Back
Full Screen
Close
Quit

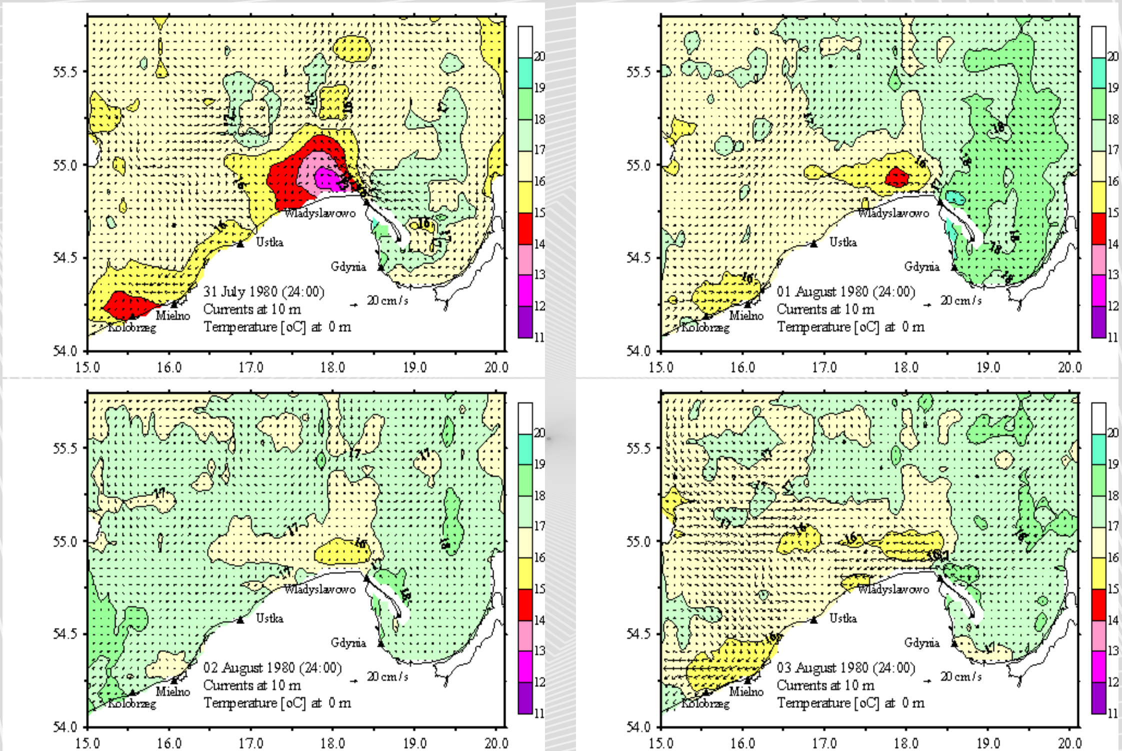

Figure 4 (... cont.) Simulated sea water temperature $[^oC]$ in surface layer and currents vector $[cm/s]$ at 10 m depth in a time sequence of 1 day from 27.07.1980 to 03.08.1980.

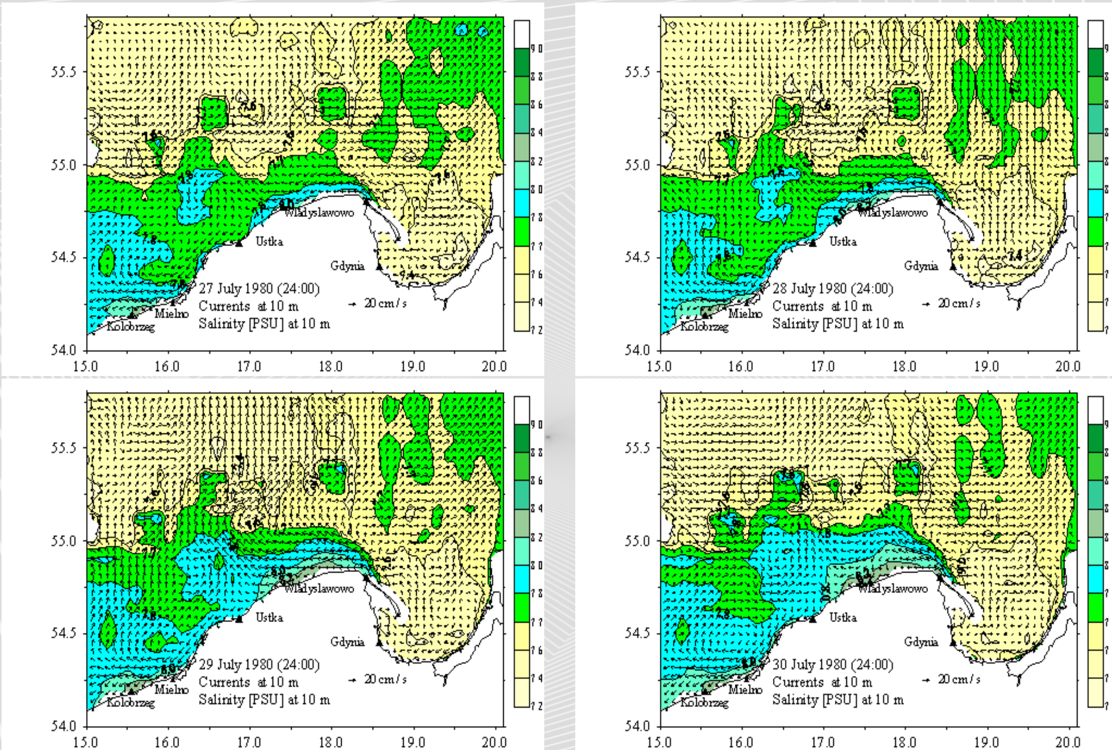

Figure 5 Simulated seawater salinity $[psu]$ and curents vectors $[cm/s]$ at 10 m in a time sequence of 1 day from 27.07.1980 to 03.08.1980.

Home Page
Title Page
Contents
Page 40 of 62
Go Back
Full Screen
Close
Quit

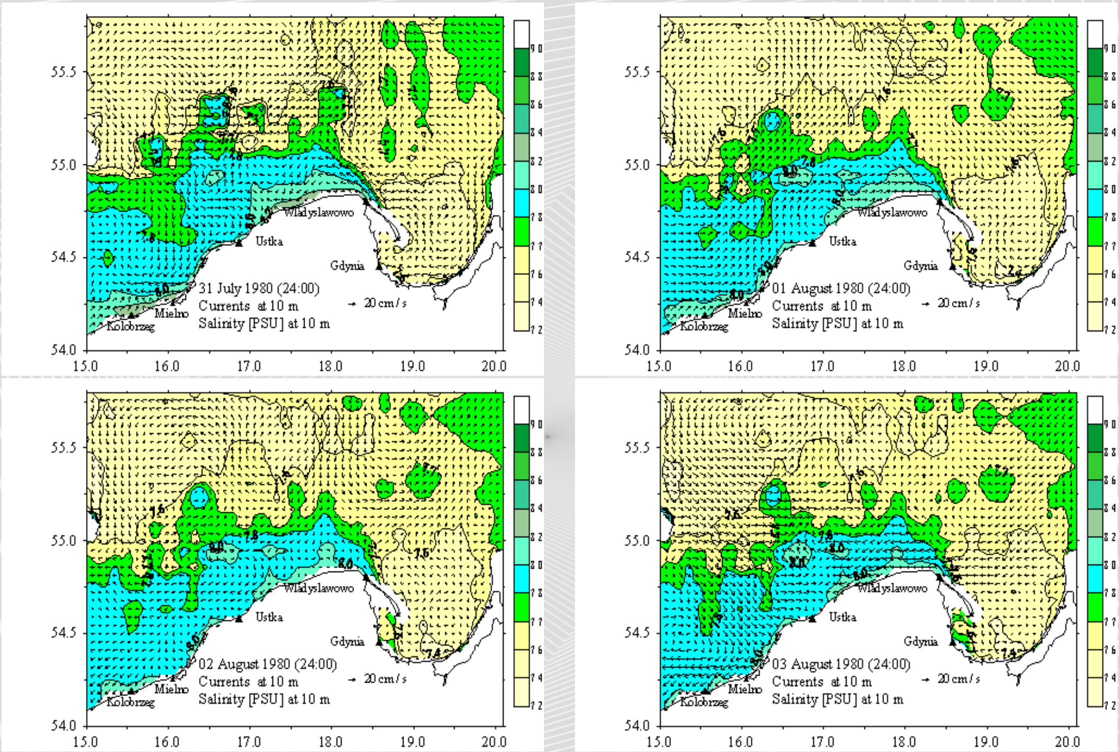

Figure 5 (... cont.) Simulated seawater salinity [psu] and curents vectors [cm/s] at 10 m in a time sequence of 1 day from 27.07.1980 to 03.08.1980.

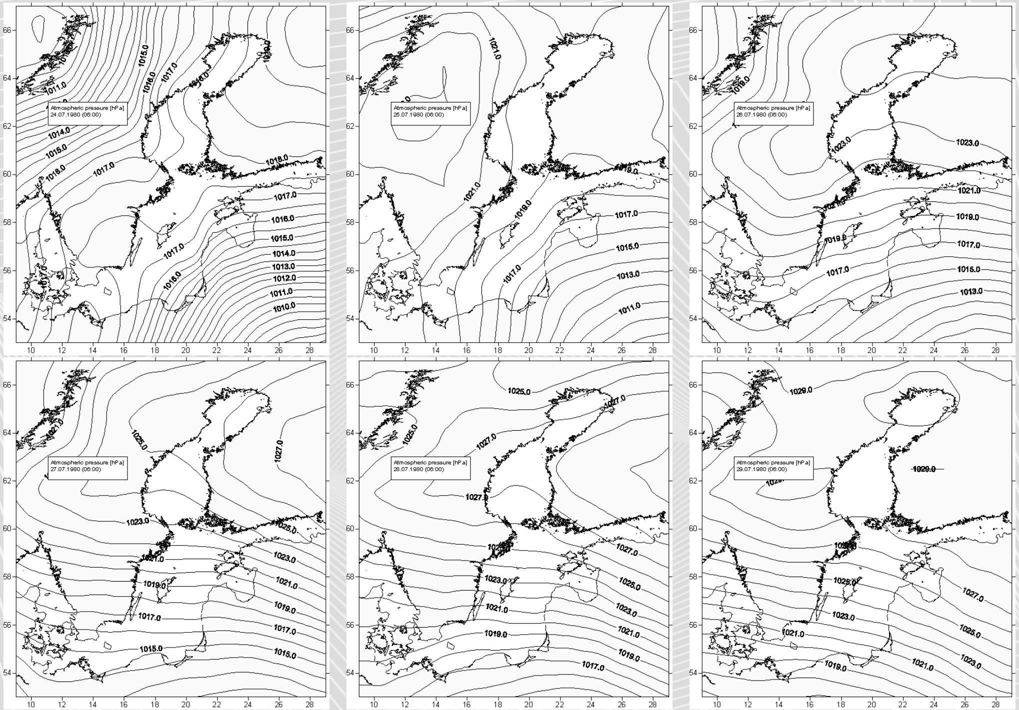

Figure 6 Anemobaric situation above the Baltic Sea in summer 1980 related to the upwelling-like event in vicinity of the Hel Peninsula (from 27.07.1980 to 03.08.1980) shown in Figs. 5 and 6. Data taken from (BED, 2000)). Isobars in [hPa].

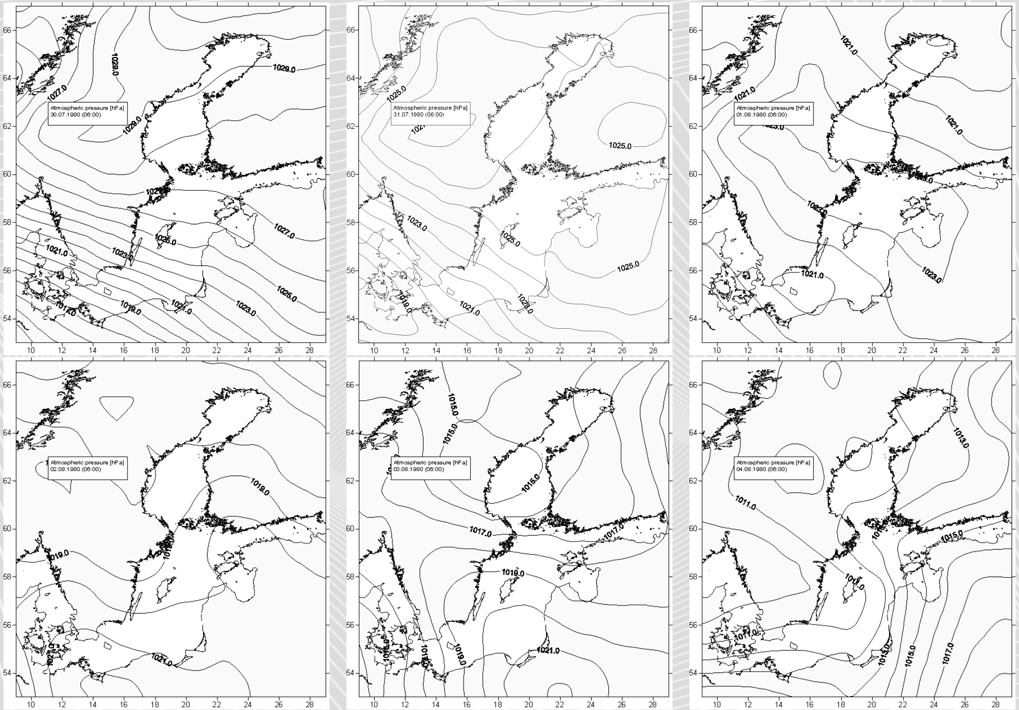

Figure 6 (... cont.) Anemobaric situation above the Baltic Sea in summer 1980 related to the upwelling-like event in vicinity of the Hel Peninsula (from 27.07.1980 to 03.08.1980) shown in Figs. 5 and 6. Data taken from (BED, 2000)). Isobars in [hPa].

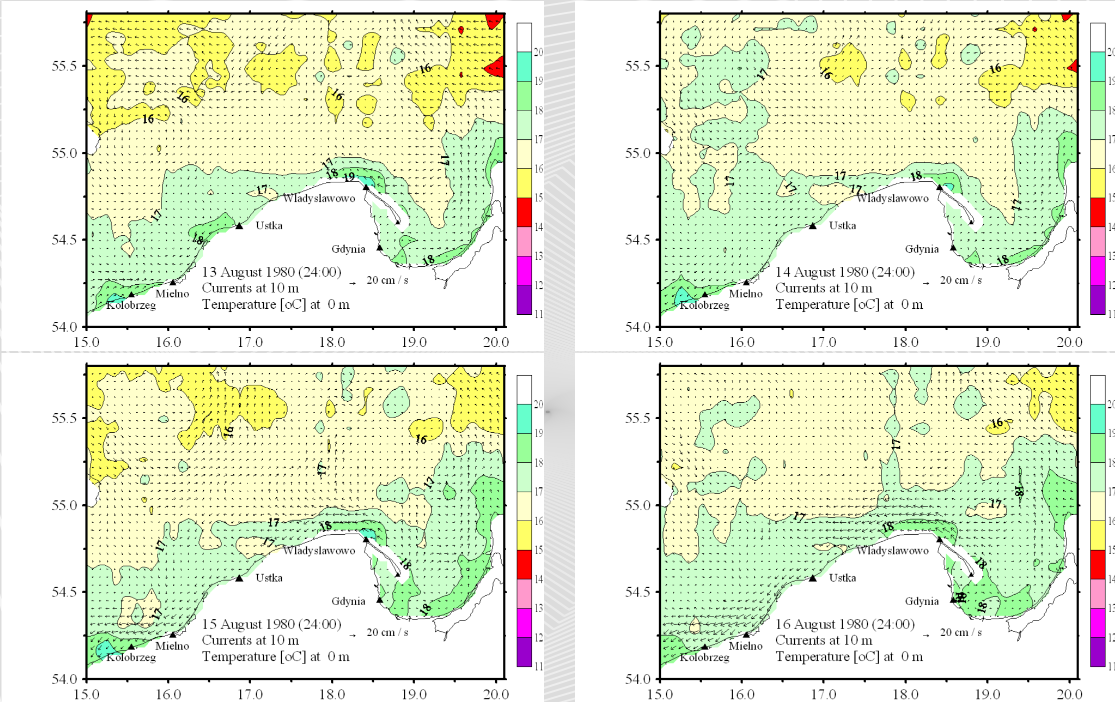

Figure 7 Simulated sea water temperature $[^oC]$ in surface layer and currents vectors $[cm/s]$ in a time sequence of 1 day from 13.08.1980 to 20.08.1980.

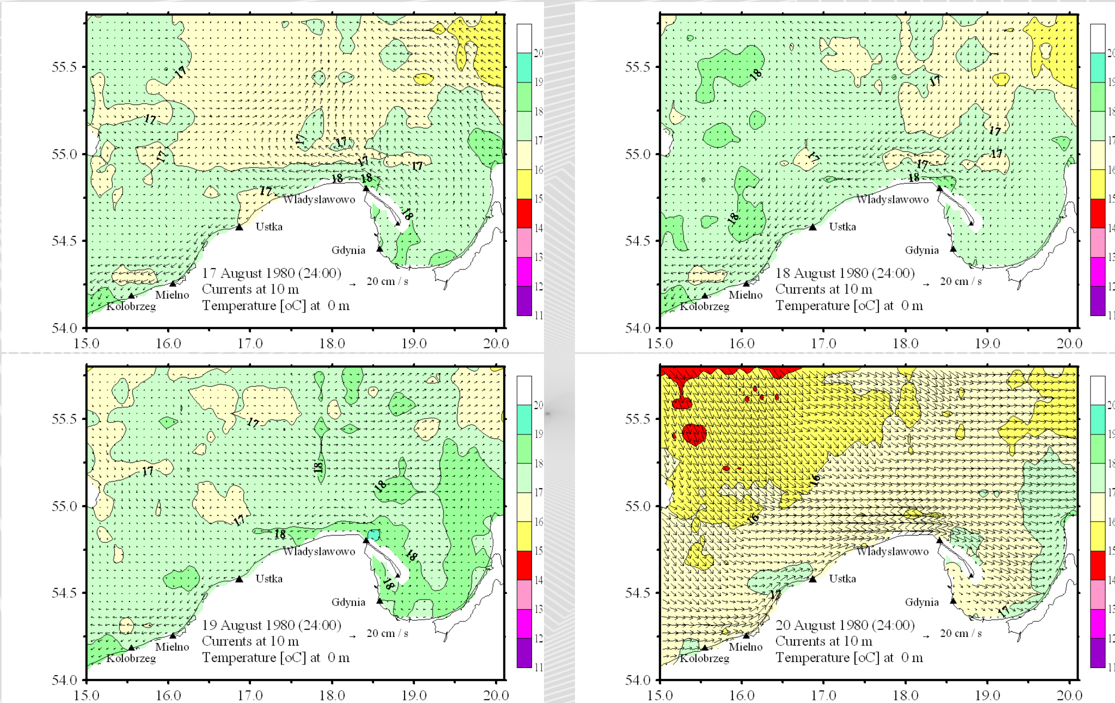

Figure 7 (... cont.) Simulated sea water temperature [^oC] in surface layer and currents vectors [cm/s] in a time sequence of 1 day from 13.08.1980 to 20.08.1980.

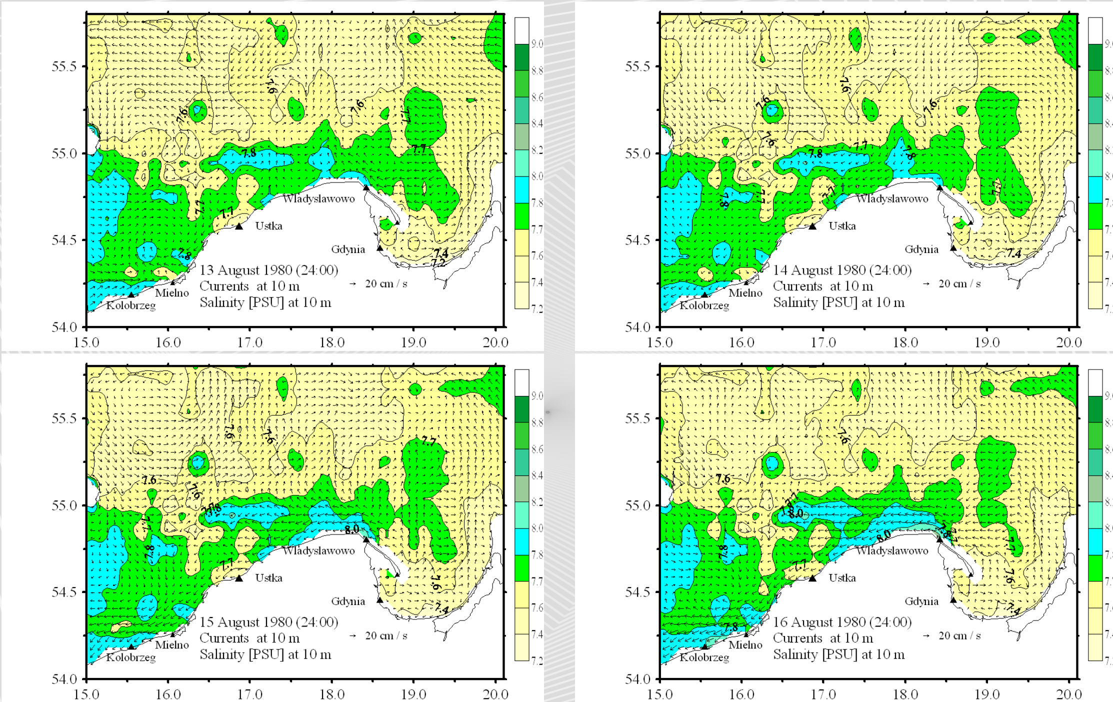

Figure 8 Simulated seawater salinity $[psu]$ and currents vector $[cm/s]$ at 10 m depth in a time sequence of 1 day from 13.08.1980 to 20.08.1980.

Home Page
Title Page
Contents
◀◀ ▶▶
◀ ▶
Page 46 of 62
Go Back
Full Screen
Close
Quit

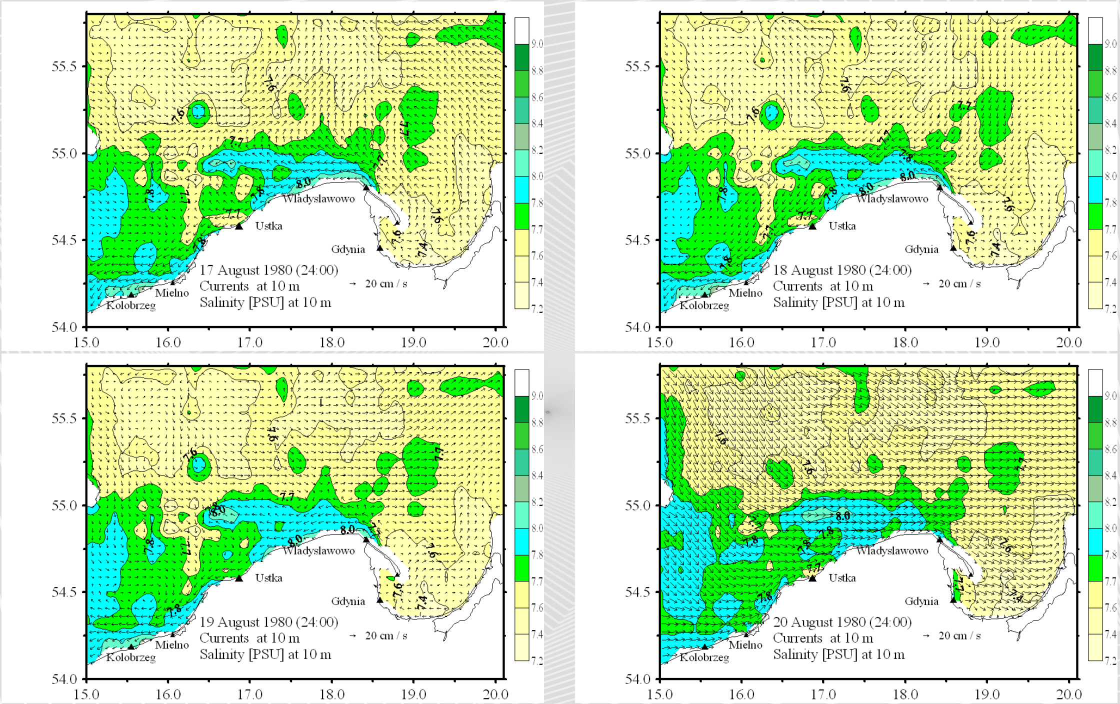

Figure 8 (... cont.) Simulated seawater salinity [psu] and currents vector [cm/s] at 10 m depth in a time sequence of 1 day from 13.08.1980 to 20.08.1980.

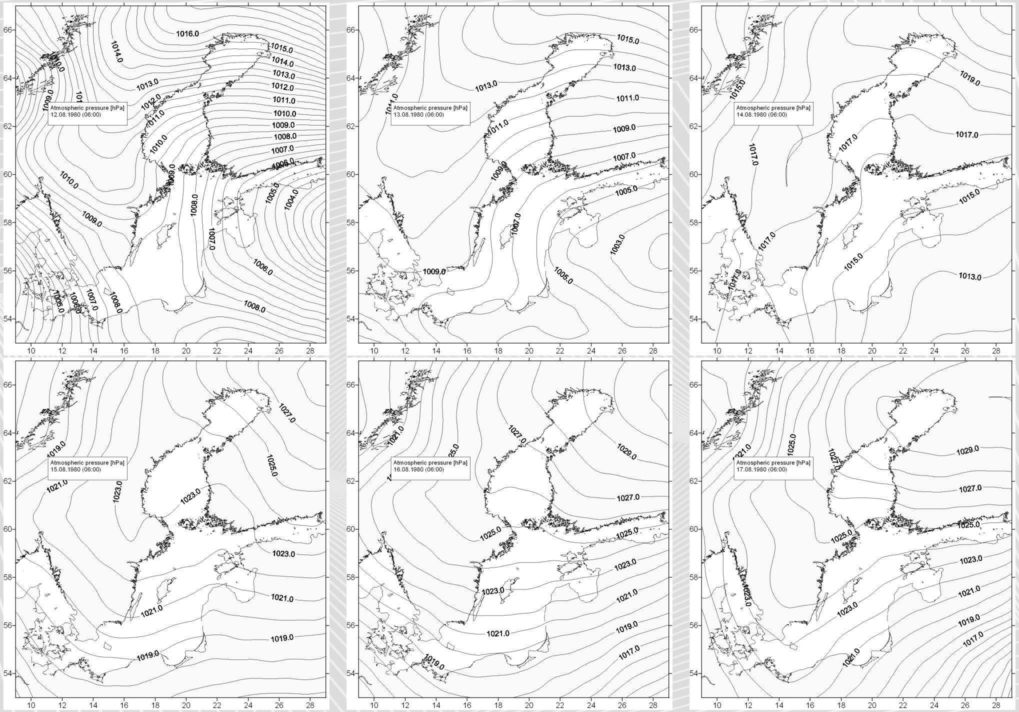

Figure 9 Anemobaric situation above the Baltic Sea in summer 1980 related to the upwelling-like event in vicinity of the Hel Peninsula (from 13.08.1980 to 20.08.1980) shown in Figs. 7 and 8. Data taken from (BED, 2000)). Isobars in [hPa].

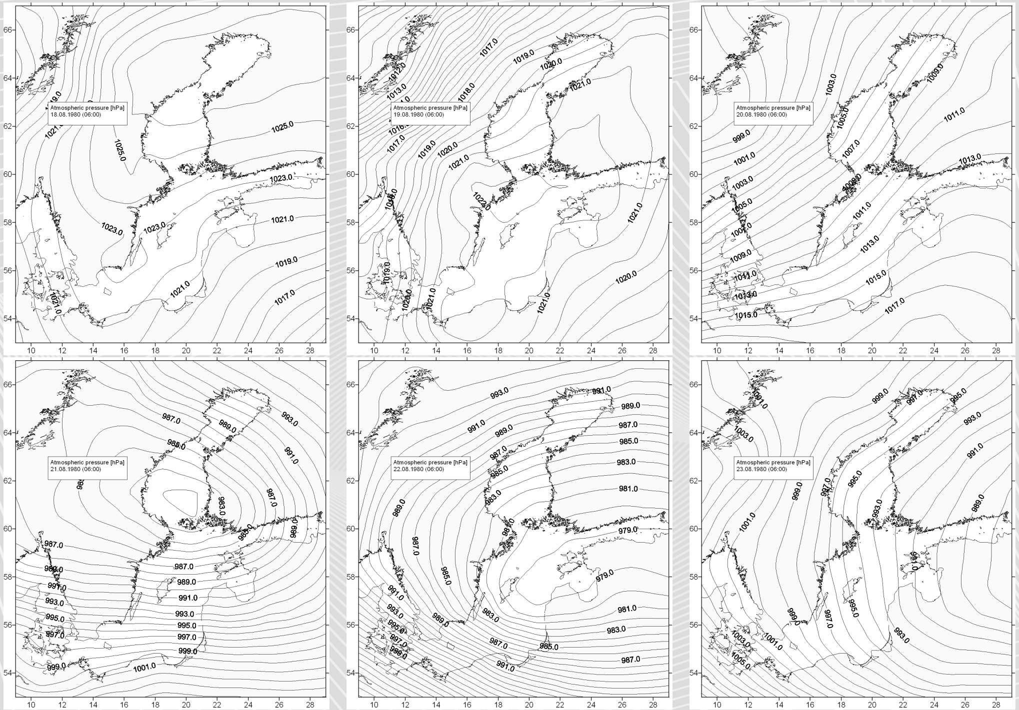

Figure 9 (... cont.) Anemobaric situation above the Baltic Sea in summer 1980 related to the upwelling-like event in vicinity of the Hel Peninsula (from 13.08.1980 to 20.08.1980) shown in Figs. 7 and 8. Data taken from (BED, 2000)). Isobars in [hPa].

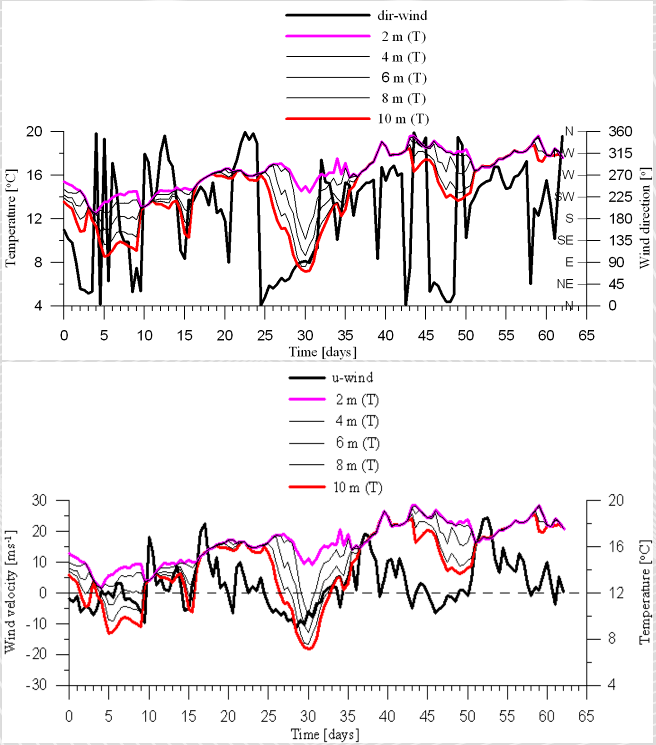

Figure 10a Time series of the longitudinal component of the wind vector speed (u) $[m/s]$ and wind direction $[^o]$ and timee series of seawater temperature T $[^oC]$ at selected depths in the point **W** off Wladyslawowo, (real atmospheric forcings for summer period, July-August, 1980). Location of point - see Fig. 1.

Home Page
Title Page
Contents
Page 50 of 62
Go Back
Full Screen
Close
Quit

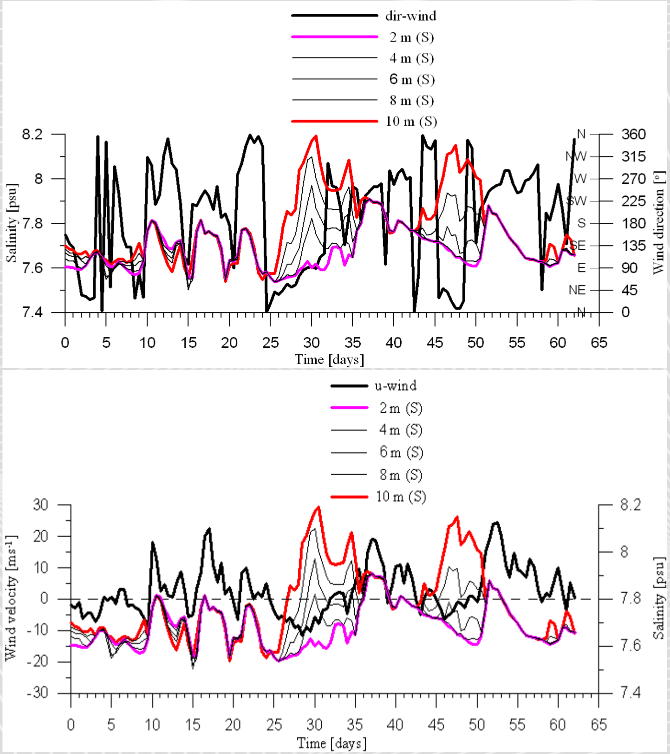

Figure 10b Time series of the longitudinal component of the wind vector speed (u) $[m/s]$ and wind direction $[^o]$ and timee series of seawater salinity S $[psu]$ at selected depths in the point **W** off Wladyslawowo, (real atmospheric forcings for summer period, July-August, 1980). Location of point - see Fig. 1.

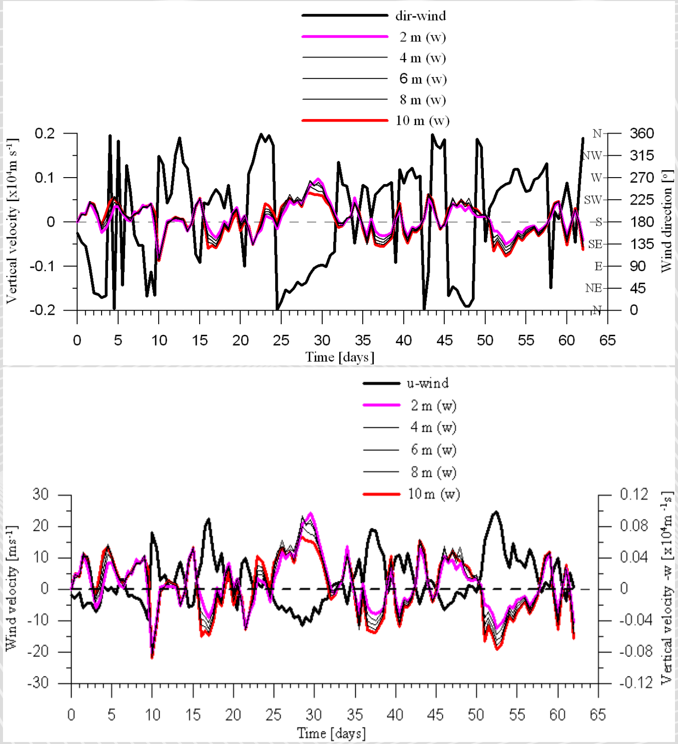

Figure 10c Time series of the longitudinal component of the wind vector speed (u) $[m/s]$ and wind direction $[^o]$ and timee series of the vertical component of currents velocity vector w $[cm/s]$ at selected depths in the point **W** off Wladyslawowo, (real atmospheric forcings for summer period, July-August, 1980). Location of point - see Fig. 1.

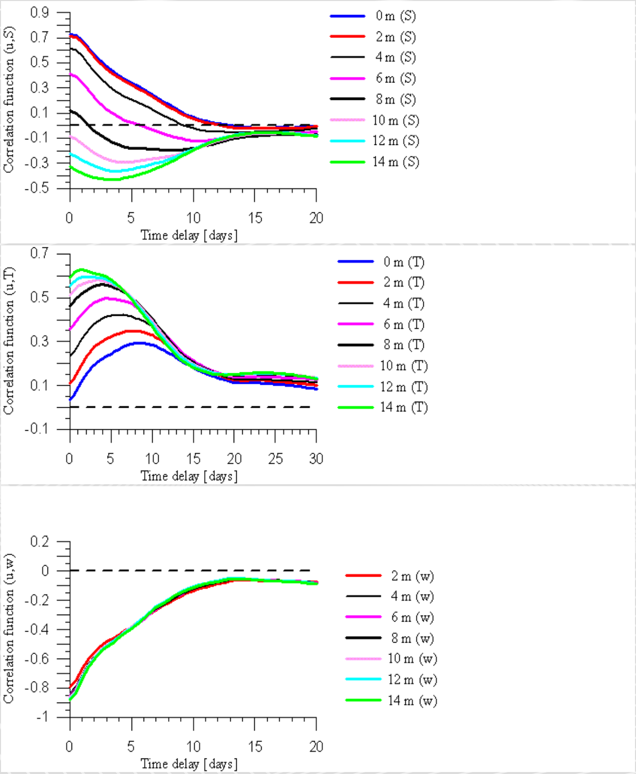

Figure 11a Cross-correlation function between the time series of longitudinal wind speed vector component (u-component) and the time series of modelelled seawater salinity S at the selected depths in the point **W** off Wladyslawowo, (real atmospheric forcings for summer period, July-August, 1980). Location of point - see Fig. 1.

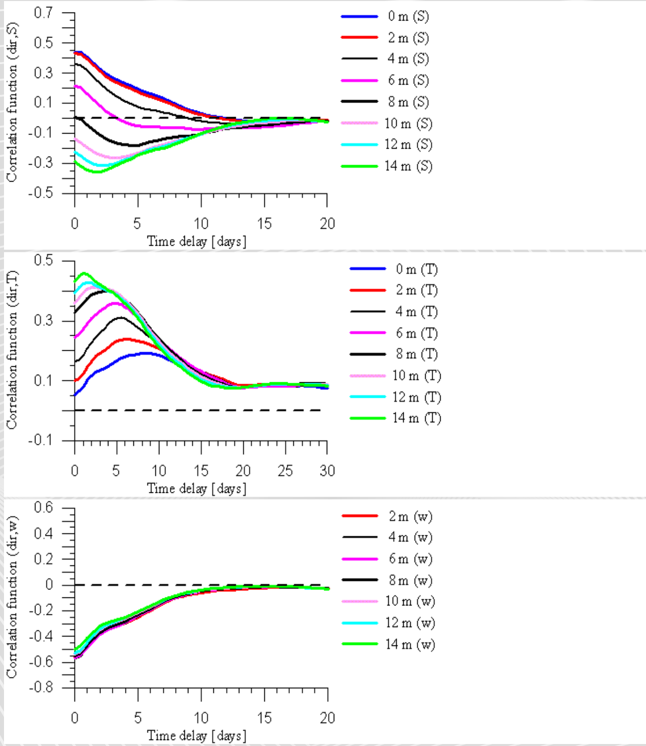

Figure 11b Cross-correlation function between the time series of wind direction and the time series of modelelled vertical component of currents velocity vector w at the selected depths in the point **W**, off Wladyslawowo, (real atmospheric forcings for summer period, July-August, 1980). Location of point - see Fig. 1.

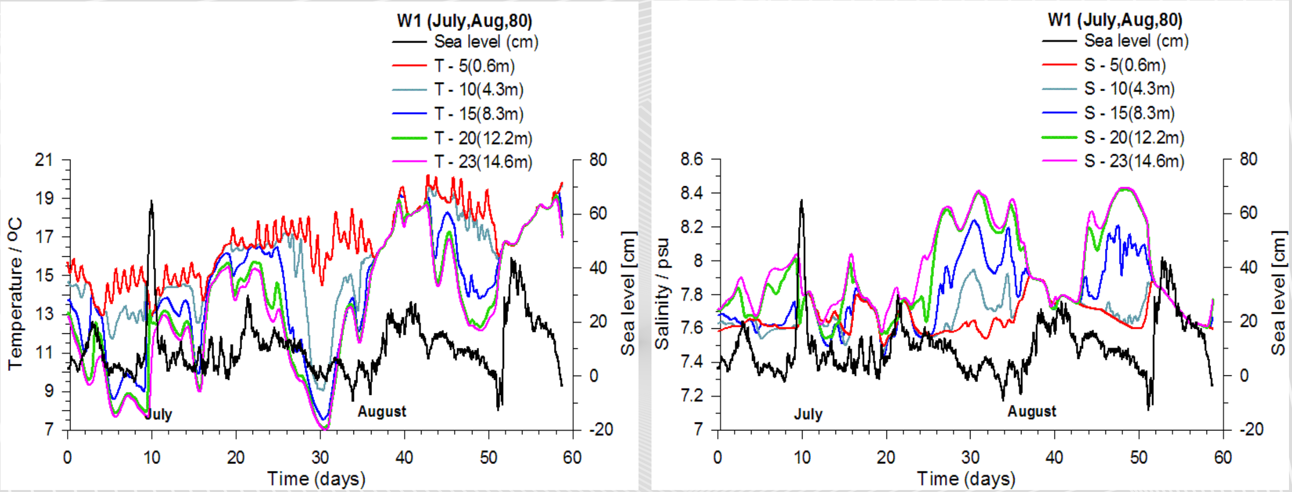

Figure 12a Time series of the modelled sea level η $[cm]$ and time series of seawater temperature T $[^oC]$ and salinity S $[psu]$ at selected depths in the point **W1** off Wladyslawowo, (real atmospheric forcings for summer period, July-August, 1980). Location of point - see Fig. 1.

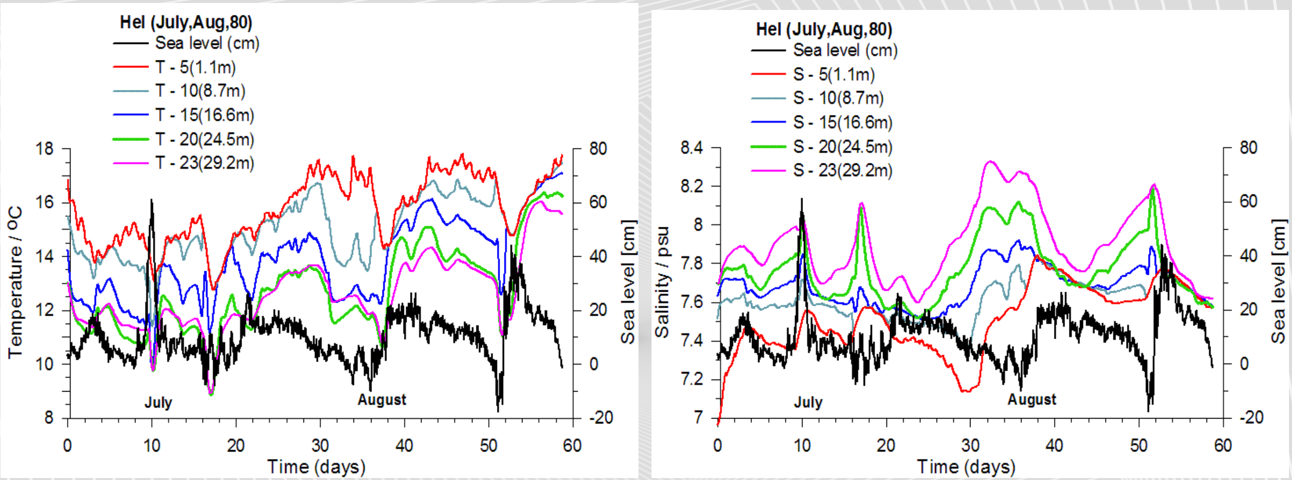

Figure 12b Time series of the modelled sea level η $[cm]$ and time series of seawater temperature T $[^oC]$ and salinity S $[psu]$ at selected depths in the point **H** off Hel, (real atmospheric forcings for summer period, July-August, 1980).Location of point - see Fig. 1.

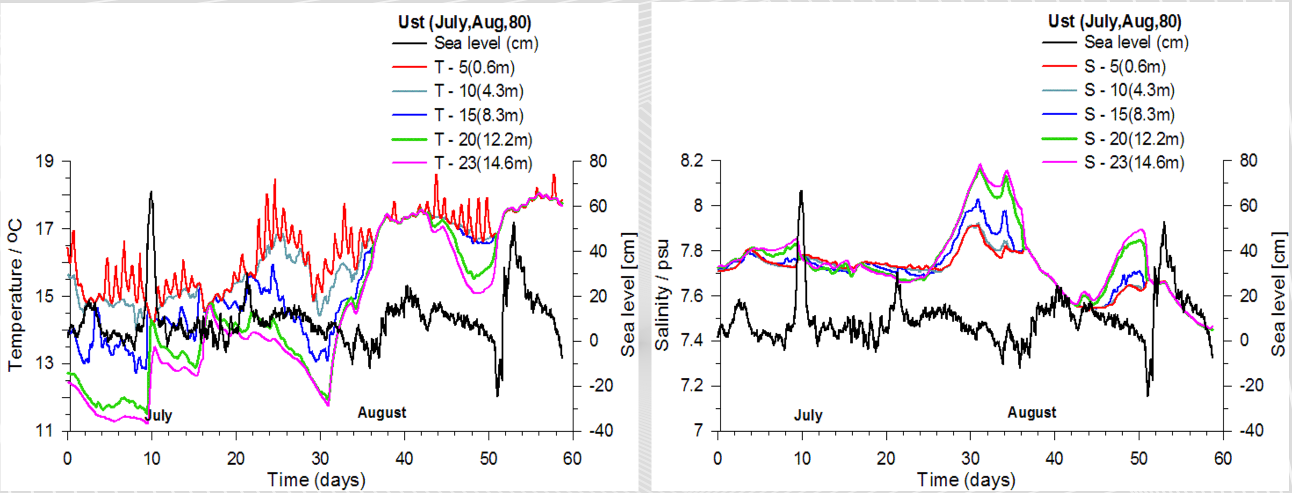

Figure 12c Time series of the modelled sea level η $[cm]$ and time series of seawater temperature T $[^oC]$ and salinity S $[psu]$ at selected depths in the point **U** off Ustka, (real atmospheric forcings for summer period, July-August, 1980).Location of point - see Fig. 1.

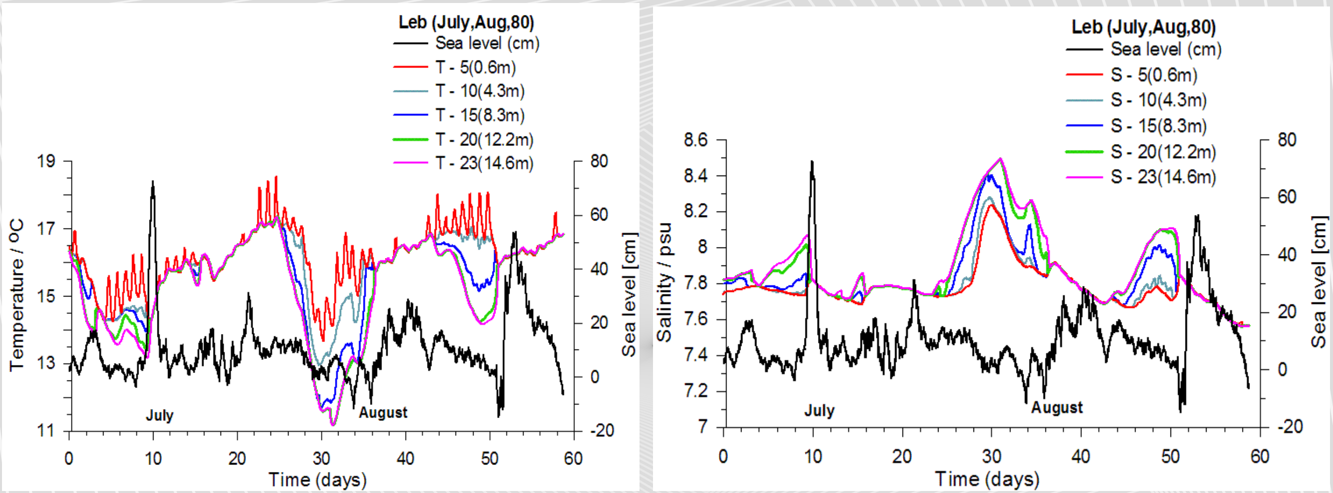

Figure 12d Time series of the modelled sea level η $[cm]$ and time series of seawater temperature T $[^oC]$ and salinity S $[psu]$ at selected depths in the point **L** off leba, (real atmospheric forcings for summer period, July-August, 1980).Location of point - see Fig. 1.

Tables caption

Table 1
Values of statistical criteria calculated for verification of modelled temperature profiles in selected points in the south-eastern Baltic Sea. See text and **Appendix** for more detail explanations

Table 2
Values of statistical criteria calculated for verification of modelled salinity profiles in selected points in the south-eastern Baltic Sea. See text and **Appendix** for more detail explanations

Table 3
Cross-correlation coefficients cor and cor_{max} between time-series of the longitudinal component of the wind vector speed (u) and wind direction and timee series of modelloed water temperature, salinity and the vertical component of the velocity vector for the current at the selected depths at the monitoring point **W**, off Wladyslawowo. In parentheses is the value of the delay(lag) (in days) for which the cross-correlation function approaches its extreme value. The calculation was carried out with the real forces forcing fields.

Table 4
Correlation coefficient $cor_{T\eta}$ i $cor_{S\eta}$ between the modelled time series of sea level η and time series of seawater temperature (T) and salinity (S) at the selected depths in the four points located in the coastal zone: **W1** (15 m), **U** (15 m), **L** (15 m), **H** (30 m). In parentheses is shown the bottom depth in the point location.

Figures captions

Figure 1 The study area and location of points used for verification of the model calculations: **S1-S5** and to visualize the results of calculations: **W, W1, H, L, U** - Wladyslawowo (**W, W1**), Hel (**H**), Leba (**L**) and Ustka (**U**), respectively; Bottom topography was elaborated based on data from Seifert and Kayser (1995). The numbers on the isolines indicate the depth in meters.

Figure 2a Modelled and in situ measured vertical distributions of temperature [^oC] and salinity [psu] at the hydrographic stations **S1** and **S2**. For details of their locations, see Fig. 1

Figure 2b Modelled and in situ measured vertical distributions of temperature [^oC] and salinity [psu] at the hydrographic stations **S3**, **S4** and **S5**. For details of their locations, see Fig. 1

Figure 3 Time evolution of wind direction [^{o}], wind velocity [m/s], the simulated seawater temperature (T) [^oC], salinity (S) [psu] and the vertical component of the currents velocity vector (w) [cm/s] at point **W** in the vicinity of the Hel Peninsula. Location of point see Fig. 1

Figure 4 Simulated sea water temperature [^oC] in surface layer and currents vector [cm/s] at 10 m depth in a time sequence of 1 day from 27.07.1980 to 03.08.1980.

Figure 5 Simulated seawater salinity [psu] and curents vectors [cm/s] at 10 m in a time sequence of 1 day from 27.07.1980 to 03.08.1980.

Figure 6 Anemobaric situation above the Baltic Sea in summer 1980 related to the upwelling-like event in vicinity of the Hel Peninsula (from 27.07.1980 to 03.08.1980) shown in Figs. 5 and 6. Data taken from (BED, 2000)). Isobars in [hPa].

Figures captions ... continued

Figure 7 Simulated sea water temperature [^oC] in surface layer and currents vectors [cm/s] in a time sequence of 1 day from 13.08.1980 to 20.08.1980.

Figure 8 Simulated seawater salinity [psu] and currents vector [cm/s] at 10 m depth in a time sequence of 1 day from 13.08.1980 to 20.08.1980.

Figure 9 Anemobaric situation above the Baltic Sea in summer 1980 related to the upwelling-like event in vicinity of the Hel Peninsula (from 13.08.1980 to 20.08.1980) shown in Figs. 7 and 8. Data taken from (BED, 2000)). Isobars in [hPa].

Figure 10a Time series of the longitudinal component of the wind vector speed (u) [m/s] and wind direction [^{o}] and timee series of seawater temperature T [^oC] at selected depths in the point **W** off Wadysawowo, (real atmospheric forcings for summer period, July-August, 1980). Location of point - see Fig. 1.

Figure 10b Time series of the longitudinal component of the wind vector speed (u) [m/s] and wind direction [^{o}] and timee series of seawater salinity S [psu] at selected depths in the point **W** off Wadysawowo, (real atmospheric forcings for summer period, July-August, 1980). Location of point - see Fig. 1.

Figure 10c Time series of the longitudinal component of the wind vector speed (u) [m/s] and wind direction [^{o}] and timee series of the vertical component of currents velocity vector w [cm/s] at selected depths in the point **W** off Wadysawowo, (real atmospheric forcings for summer period, July-August, 1980). Location of point - see Fig. 1.

Figures captions ... continued

Figure 11a Cross-correlation function between the time series of longitudinal wind speed vector component (u-component) and the time series of modelelled seawater salinity S at the selected depths in the point **W** off Wladyslawowo, (real atmospheric forcings for summer period, July-August, 1980). Location of point - see Fig. 1.

Figure 11b Cross-correlation function between the time series of wind direction and the time series of modelelled vertical component of currents velocity vector w at the selected depths in the point **W**, off Wladyslawowo, (real atmospheric forcings for summer period, July-August, 1980). Location of point - see Fig. 1.

Figure 12a Time series of the modelled sea level η $[cm]$ and time series of seawater temperature T $[^oC]$ and salinity S $[psu]$ at selected depths in the point **W1** off Wladyslawowo, (real atmospheric forcings for summer period, July-August, 1980). Location of point - see Fig. 1.

Figure 12b Time series of the modelled sea level η $[cm]$ and time series of seawater temperature T $[^oC]$ and salinity S $[psu]$ at selected depths in the point **H** off Hel, (real atmospheric forcings for summer period, July-August, 1980).Location of point - see Fig. 1.

Figure 12c Time series of the modelled sea level η $[cm]$ and time series of seawater temperature T $[^oC]$ and salinity S $[psu]$ at selected depths in the point **U** off Ustka, (real atmospheric forcings for summer period, July-August, 1980).Location of point - see Fig. 1.

Figure 12d Time series of the modelled sea level η $[cm]$ and time series of seawater temperature T $[^oC]$ and salinity S $[psu]$ at selected depths in the point **L** off Leba, (real atmospheric forcings for summer period, July-August, 1980). Location of point - see Fig. 1.